



A Comparative Study of the DPT and CPT in Evaluating Liquefaction Potential for Gravelly Soil at the Port of Wellington, New Zealand

Jashod Roy, M.ASCE¹; Kyle M. Rollins, M.ASCE²; Riwaj Dhakal, M.ASCE³; and Misko Cubrinovski, M.ASCE⁴

Abstract: Characterizing gravelly soil using in situ penetration testing procedures is a significant challenge for geotechnical engineers. The interaction between the penetrometer and large gravel particles can obscure the penetration resistance of the soil matrix, which is the target of the investigation, and lead to significant uncertainty regarding the properties of the soil. Hence, the size of the probe relative to the maximum particle size of the soil matrix is an important factor to consider when performing interpreting and penetration tests. In this respect, the standard penetration test (SPT) and cone penetration test (CPT) can have potential issues in measuring the penetration resistance in certain cases depending on the size and percentage of gravel particles. Recently, the Chinese dynamic cone penetration test (DPT) consisting of a larger-diameter probe with higher hammer energy has been used to develop probabilistic liquefaction triggering curves for gravelly soil. In the present study, an instructive comparison is presented between the performance of the DPT and CPT in evaluating the liquefaction potential of gravelly soils based on in situ testing at the port of Wellington in New Zealand. Gravelly reclamation fill at the port liquefied during the 2016 M_w 7.8 Kaikōura earthquake, but only limited parts of the same fill deposits manifested liquefaction during the M_w 6.6 Cook Strait and Lake Grassmere earthquakes that occurred in 2013. Triggering analyses have been performed using both DPT- and CPT-based triggering procedures to estimate the potential for liquefaction in these gravelly deposits for these three earthquake events. The CPT-based cyclic resistance ratio (CRR) profiles showed several intermittent spikes with depth due to the interaction of the small-diameter cone with large gravel particles. However, the lower range of values excluding the spikes in the CPT-based CRR profiles primarily governed the liquefaction potential of the reclamation fill, and they are in good agreement with the DPT-based CRR profiles. Both the CPT and DPT-based triggering analyses successfully estimated liquefaction manifestation during the Kaikōura event, some liquefaction manifestation during the Cook Strait event and very limited manifestation during the Lake Grassmere event, which is largely consistent with observations. DOI: 10.1061/JGGEFK.GTENG-10769. © 2023 American Society of Civil Engineers.

Practical Applications: This case history clearly shows that sandy gravel can liquefy. In this case, the sand content was high enough (>30%) to fill the pore space and reduce the permeability so that it could liquefy. For sandy gravel at Centerport, New Zealand, with D_{50} (50% finer particle size) between 3 and 10 mm, the ratio of D_{50} to penetrometer diameter (D_p) would occasionally exceed 33% to 50% for the CPT, and some artificial increase in penetration resistance would be expected. In contrast, the D_{50} to D_p ratio for the DPT would not exceed 15%, and gravel particles would not affect the DPT blow count. This assessment is borne out in the comparison between the CRR from the CPT and DPT. For example, the CRRs from the DPT were relatively constant in the sandy gravel, whereas the CRRs from the CPT showed several spikes with depth, but were otherwise consistent with those from the DPT. In some cases, the CPT cannot penetrate layers with larger or denser gravel particles. The DPT cannot identify nonliquefiable cohesive layers; therefore, samples from a companion borehole are needed to identify them. The good agreement between the CRRs from the CPT and DPT for three earthquakes confirmed the reliability of these two independently developed methods.

Author keywords: Cone penetration test (CPT); Dynamic cone penetration test (DPT); Gravelly soil; Liquefaction; Reclaimed land.

Note. This manuscript was submitted on February 1, 2022; approved on July 3, 2023; published online on August 31, 2023. Discussion period open until January 31, 2024; separate discussions must be submitted for individual papers. This paper is part of the *Journal of Geotechnical and Geoenvironmental Engineering*, © ASCE, ISSN 1090-0241.

Introduction

Over the last 128 years, gravels have liquefied at multiples sites in at least 25 different earthquakes (Rollins et al. 2021). Gravel liquefaction has also caused significant damage to ports in Greece (Athanasopoulos-Zekkos et al. 2019), Chile (Morales et al. 2020), Ecuador (Lopez et al. 2018), Kobe Port Island in Japan (Japanese Geotechnical Society 1996), and Centerport in Wellington, New Zealand (Cubrinovski et al. 2017). Many ports are constructed using gravelly soils or rockfill, which was once believed to be immune to liquefaction (Seed et al. 1976), but recent case histories clearly indicate that this is not the case. For these port facilities, assessing the potential for liquefaction and performing appropriate mitigation techniques are often multi-million-dollar issues. Ports are essential to economic activity and are critical lifelines that need to function after an earthquake event. Therefore, appropriate assessment of liquefaction potential in gravelly soils in port facilities is a critical issue.

¹Research Assistant, Dept. of Civil and Environment Engineering, Brigham Young Univ., 430 Engineering Bldg., Provo, UT 84602 (corresponding author). ORCID: https://orcid.org/0000-0003-0854-3790. Email: jashod.roy@gmail.com

²Professor, Dept. of Civil and Environment Engineering, Brigham Young Univ., 430 Engineering Bldg., Provo, UT 84602. ORCID: https://orcid.org/0000-0002-8977-6619. Email: rollinsk@byu.edu

³Research Assistant, Dept. of Civil and Natural Resources Engineering, Univ. of Canterbury, Private Bag 4800, Christchurch 8140, New Zealand. ORCID: https://orcid.org/0000-0001-8823-7130. Email: ribu.dhakal@pg.canterbury.ac.nz

⁴Professor, Dept. of Civil and Natural Resources Engineering, Univ. of Canterbury, Private Bag 4800, Christchurch 8140, New Zealand. ORCID: https://orcid.org/0000-0002-2843-8309. Email: misko.cubrinovski@canterbury.ac.nz

Liquefaction potential in sands and silty sands is typically evaluated using in situ tests such as the standard penetration test (SPT) or the cone penetration test (CPT). However, these widely used methods can become less reliable for gravelly soils, e.g., reclaimed fills that often contain inhomogeneous soils with gravel or clean gravel layers (Tokimatsu 1988), due to interference of the penetration probe with large-size gravel particles. Iqbal et al. (2004) reported that the CPT is likely to reach refusal when the D_{50} size is greater than the size of the penetrometer and that interference effects start to increase the cone resistance (q_c) when D_{50} is about one-third the size of the penetrometer. However, the SPT and CPT may be able to correctly evaluate the liquefaction potential of loose gravelly strata with low penetration resistance (Andrus 1994; Kokusho and Yoshida 1997; Rhinehart et al. 2016; Dhakal et al. 2020a).

In addition, the CPT may be successful in evaluating gravelly deposits that are composed of gravel-sand-silt mixtures where the finer fractions (silt and sand) significantly influence the behavior of the entire soil strata (Cubrinovski et al. 2018; Dhakal et al. 2020b). Nevertheless, in medium-dense to dense layers consisting of largesize particles, the cone may not successfully penetrate, making it necessary to drill through the layer to continue advancing the cone through the remainder of the depth. Sometimes, as the penetration resistance at a site increases, it becomes increasingly difficult to determine if the increased resistance is because of the increased density of the soil strata or because of interference with large particles. Due to the influence of large particles, penetration resistance may even reach refusal in some cases when the soil is not particularly dense (Cao et al. 2013; Rollins et al. 2020). These phenomena produce uncertainty regarding the liquefaction evaluation of gravelly sites using these standard testing methods.

With a diameter of 168 mm, the Becker penetration test (BPT) provides an alternative testing method with a much larger diameter to particle size ratio, which is a desirable attribute for minimizing gravel size effects on penetration resistance. Unfortunately, there are presently no direct correlations between BPT blow count and liquefaction resistance. Therefore, the BPT blow count must be correlated with the SPT blow count based on correlations in sands (Sy and Campanella 1994; Harder 1997; DeJong et al. 2017; Chowdhury et al. 2021) to assess liquefaction resistance. This indirect liquefaction correlation adds uncertainty to the process of assessing liquefaction potential. Furthermore, the BPT is simply not available in most of the world, as is the case in New Zealand.

The dynamic cone penetration test (DPT), developed in China to measure the penetration resistance of gravels, provides another alternative approach for assessing liquefaction in gravels. The DPT employs a relatively simple penetrometer consisting of a 74-mm-diameter cone tip driven by a 120-kg hammer with a free-fall height of 100 cm using a 60-mm drill rod that reduces skin friction on the rods. At 74 mm, the DPT diameter is 50% larger than the SPT and 110% larger than a standard 10-cm² CPT, which makes the equipment more effective in penetrating medium to coarse gravels to produce meaningful evaluations of soil resistance.

One major advantage of the DPT over the BPT is that the DPT equipment can be easily fabricated and made available at any location around the world. However, the 60-mm rod and 74-mm cone tip leave a 7-mm gap that can be subject to skin friction due to loose soil collapsing during the DPT penetration below the water table. This frictional resistance, although relatively small compared with a straight-sided probe, adds to the overall DPT resistance because there is no systematic method to account for the skin friction exclusively. Also, unlike the CPT, the DPT does not provide correlations to identify soil behavior type. Therefore, a separate

borehole is required to identify soil stratigraphy and define gradation properties.

Cao et al. (2013) directly correlated the DPT resistance with the liquefaction potential of gravelly soil based on 47 liquefaction case histories from the Chengdu Plain in China during the M_w 7.9 Wenchuan earthquake in 2008. Cao et al. (2013) also reported that the DPT can often penetrate cobbly gravels, eliminating the need to drill through them, although the penetration resistance may still be artificially increased. More recently, Rollins et al. (2021) developed DPT-based triggering curves based on an expanded data set consisting of 137 liquefaction case histories from seven different countries during 10 different earthquakes in a variety of depositional environments. These probabilistic DPT-based liquefaction triggering curves are shown in Fig. 1, where liquefaction case histories are indicated by solid circles and no liquefaction manifestation case histories are shown by open circles.

The liquefaction case histories at Centerport in Wellington, New Zealand, provide an important opportunity for comparing the performance of the DPT and the conventional CPT for predicting the liquefaction behavior of gravelly soil. Centerport has been subjected to three significant seismic events recently, namely the M_w 7.8 Kaikōura earthquake of 2016, along with the M_w 6.6 Cook Strait and the M_w 6.6 Lake Grassmere earthquakes, both in 2013. Out of these, the Kaikōura event produced widespread liquefaction of the reclaimed land, causing significant damage to existing structures along with lateral spreading and seismic settlement (Cubrinovski et al. 2017). In contrast, the Cook Strait and Lake Grassmere events did not produce significant liquefaction or any severe damage except for the occurrence of minor ground cracking and differential ground movement in isolated locations and partial collapse and movement of the ground toward the sea at the south end of the port (Dhakal et al. 2020b).

To characterize the liquefaction potential of the gravelly soil deposits at the reclaimed land, comprehensive site exploration programs were carried out by conducting 92 CPTs in reclaimed gravelly soil, the majority of which were performed in locations of severe liquefaction damage with significant volumes of sand and gravel ejecta observed (Cubrinovski et al. 2017; 2018; Dhakal et al. 2020a). Based on these CPT tests and adjacent boreholes, subsurface soil profiles were developed and liquefaction resistance in the gravelly soil deposits was evaluated (Dhakal et al. 2020a) for these three seismic events using an existing CPT-based triggering procedure (Boulanger and Idriss 2014). Dhakal et al. (2020b) illustrated the applicability of existing CPT-based procedures developed primarily for sands for the Centerport gravelly fill.

In this study, DPT tests were performed at several locations adjacent to CPTs performed by Dhakal et al. (2020b) to characterize the liquefaction potential of gravelly soils using the newly developed liquefaction triggering procedure based on DPT testing (Rollins et al. 2021). As a part of this study, some of the results obtained from the two different methods (DPT and CPT) for the same locations at the reclamation site have been thoroughly examined to draw a clear comparison between the performance of the CPT and DPT in evaluating the liquefaction potential of the gravelly soil. In this context, the characteristics of the reclamation site, details of the earthquake events, and the observed features of liquefaction manifestation are briefly described to provide relevant background. Finally, the results of the site exploration program and corresponding liquefaction resistance analysis are discussed in detail, followed by an instructive comparison between the performance of DPT and CPT in assessing the liquefaction potential of gravelly soil.

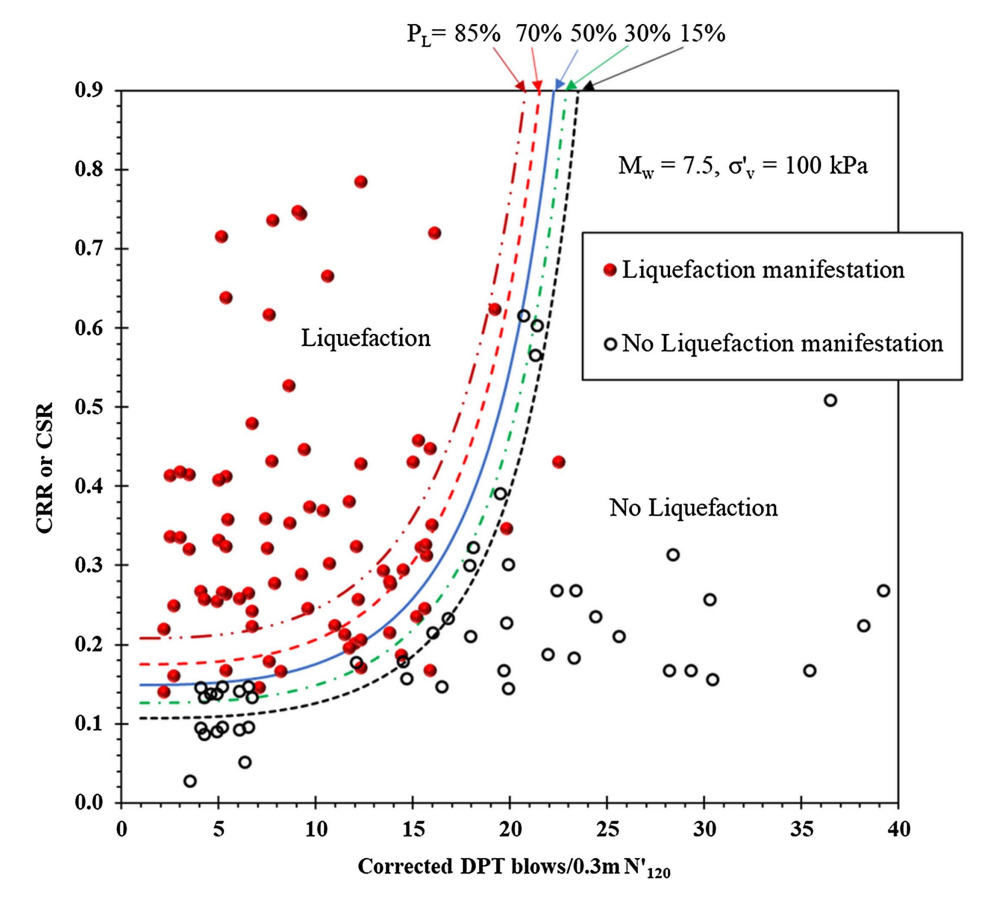


Fig. 1. DPT-based liquefaction triggering curves for gravelly soil. (Data from Rollins et al. 2021.)

Site Description

Centerport is situated near central Wellington in New Zealand. The port was developed by three different phases of land reclamation over the last 170 years after European settlement in the 1850s (Semmens et al. 2010). The latest reclamation work performed during 1965–1976 is known as the Thorndon reclamation, which has been investigated in the present study. An aerial view of different parts of the reclaimed lands along with the construction periods and the buried seawall are shown in Fig. 2 (Dhakal et al. 2020a).

The Thorndon reclamation was primarily constructed by end-dumping of gravelly soils transported from quarries in the Wellington region. The fill material at the Thorndon reclamation is primarily composed of gravelly soil (>50% gravel size particles) mixed with sand and silt fractions (>30%). The gravelly soils at the southern side of the seawall are approximately 40 years old, whereas the similar end-tipped gravelly reclamation north of old seawall is about 100 years old.

The subsurface profile at the Thorndon reclamation consists of a 2–3-m-thick compacted earth fill layer from the ground surface. The groundwater table generally fluctuates within 1 m below the base of the compacted fill. This earth fill was compacted to support the asphalt pavement and a base course layer, which was necessary for port operations. Below the compacted fill, the end-dumped sandy gravel deposit is uncompacted and extends to a depth of approximately 10 to 22 m. Along the edge of the slope near the coastline, this uncompacted reclamation fill was covered by a rock fill layer to provide coastal protection. Underlying the reclamation fill is a thin Holocene beach layer and marine sediments comprised of interbedded sand, clay, silty clay, and soft

to very stiff clay having a thickness of 1 to 4 m. This layer is in turn underlain by 100-m-thick weathered Pleistocene sediments (Wellington Alluvium) consisting of interbedded dense gravel and stiff to very stiff silt. Underlying this alluvium, there is Greywacke sandstone/siltstone bedrock estimated to begin at a depth of 100 to 150 m. The upper 25 m of the subsurface soil profile at the Thorndon reclamation is shown schematically in Fig. 3 (Dhakal et al. 2020a).

Prior to the earthquake events, extensive SPT samplings were performed (27 boreholes in about 12 locations) at Centerport (Tonkin & Taylor 2006, 2012, 2014) to investigate the subsurface soil profiles. After the Kaikōura earthquake, more samples were collected from the ejecta and SPT boreholes. The range of grainsize distribution curves for the reclamation fill and marine deposits obtained from the SPT investigations are shown in Fig. 4 (Cubrinovski et al. 2017). Some of the previous SPT boreholes located near the CPT and DPT holes of the present study are shown in Fig. 5.

The gradation curves corresponding to these boreholes are also plotted in Fig. 4. All these gradation curves delineate that the subsurface deposit is composed of gravelly soil with 45% to 70% gravel (4.75-mm criterion), 15% to 40% sand, and fines content of less than 15%. In the fill material, the fines fraction mainly contained nonplastic silt material. In contrast, samples from marine deposits were found to be predominantly sandy soil with fines content ranging between 15% and 35%, where the fines content has both silt and clay fractions. The median grain size (D_{50}) of the gravelly fill was observed to be between 3 and 10 mm, whereas it was about 0.2–0.3 mm for the marine deposits. Besides the gradation curves, an average distribution of gravel content versus depth has

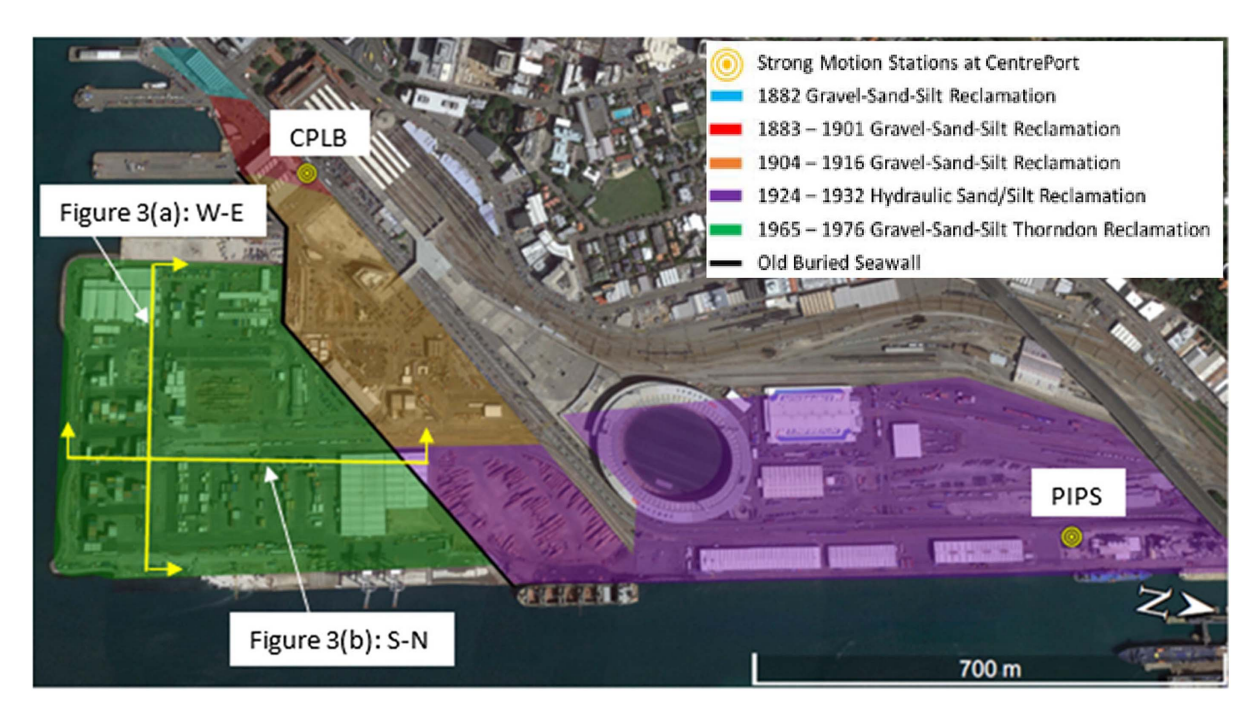


Fig. 2. Aerial view of Centerport showing reclamation zones, old-buried seawall, location of strong motion stations CPLB and PIPS, and transects of cross-sections shown in Fig. 3. (Adapted from Dhakal et al. 2020a.)

also been plotted in Fig. 4 based on the SPT sampling data collected from the entire port area. Overall, the gravelly fill material was found to be relatively consistent throughout the entire reclamation area without any significant variation in the gravel content shown in Fig. 4. More detailed descriptions and characterization of the soil deposits at the Centerport have been given by Cubrinovski et al. (2017) and Dhakal et al. (2020b).

Brief History of the Seismic Events

The M_w 7.8 Kaikōura earthquake occurred on November 14, 2016, on the South Island of New Zealand. The source-to-site distance $R_{\rm RUP}$ (i.e., the closest distance between the causative faults and Centerport) was approximately 60 km (Cubrinovski et al. 2018). Ground motions were recorded at several strong motion stations (SMS) in the vicinity of the port, which included a rock site, natural soil deposits, shallow reclaimed sites, and deep reclaimed land sites in an area of rapidly changing geometry and depth to bedrock. Two SMS were installed in the reclaimed land at Centerport, namely CPLB and PIPS. As shown in Fig. 2, CPLB was installed in the gravelly fill near the Thorndon reclamation and PIPS was installed on the hydraulically filled reclaimed area. According to these SMS records, the Kaikōura event produced ground shaking with horizontal geometric mean peak ground accelerations (PGAs) of 0.25g and 0.24g at CPLB and PIPS, respectively.

In 2013, the North and South Islands of New Zealand were hit by a sequence of two significant seismic events, namely, Cook Strait and Lake Grassmere. The Cook Strait event occurred on July 21, 2013, and the Lake Grassmere event took place on August 16, 2013. Both events were assigned moment magnitudes of 6.6 (Holden et al. 2013; Morris et al. 2013). The source-to-site distance $R_{\rm RUP}$ was 44 km for the Cook Strait event and 65 km for the Lake Grassmere event (Tonkin & Taylor 2014). Based on the ground motion recordings, the Cook Strait earthquake generated PGAs of 0.22g at the CPLB station and the Lake Grassmere event produced PGAs of 0.15g and 0.11g at CPLB and PIPS, respectively.

The duration of these two events were substantially shorter than the Kaikōura event (Cubrinovski et al. 2018), having a smaller number of significant cycles. All the earthquake parameters for all three events are briefly summarized in Table 1.

CPLB and PIPS were not located within the Thorndon reclamation, and thus records were not directly obtained from the top of the gravelly fill deposits that liquefied during the Kaikōura earthquake. However, the two SMS are located on reclaimed land sites around 75 and 900 m from the buried seawall, respectively (Fig. 2). Hence, the recorded ground motions (intensity, duration, and PGAs) include the site amplification effects based on native and reclaimed soil deposits of different thickness and basin-edge effects involving various bedrock depth and geometry (Cubrinovski et al. 2018). The inclusion of local soil amplification effects by ground response analysis generated similar ground motion characteristics for Kaikōura and Lake Grassmere events as recorded from the SMS (Bradley et al. 2017, 2018). These PGAs do not reflect any effect of partial base isolation due to the occurrence of liquefaction at the reclamation sites. Hence, the recorded results seem to be reliable in representing the characteristics of the seismic events used in the present study. The effects of PGA variation for CPT-based liquefaction assessment within the port are not considered in this paper.

Port Performance during Earthquake Events

Following the Kaikōura event, a QuakeCore-geotechnical extreme event reconnaissance (GEER) survey was conducted at Centerport on November 17, 2016, when most of the liquefaction features still existed on the ground surface at the reclamation site (Cubrinovski et al. 2017). Based on the survey report, widespread liquefaction was observed at the end-dumped reclamation fill in the form of soil ejecta, lateral and vertical ground movements, and cracks and fissures, especially along the interface zones of wharves and buildings. Fig. 5 schematically shows a map of liquefaction ejecta on the pavement surface of the port at the Thorndon reclamation. The ejected soils in this area predominantly consisted of gravelly

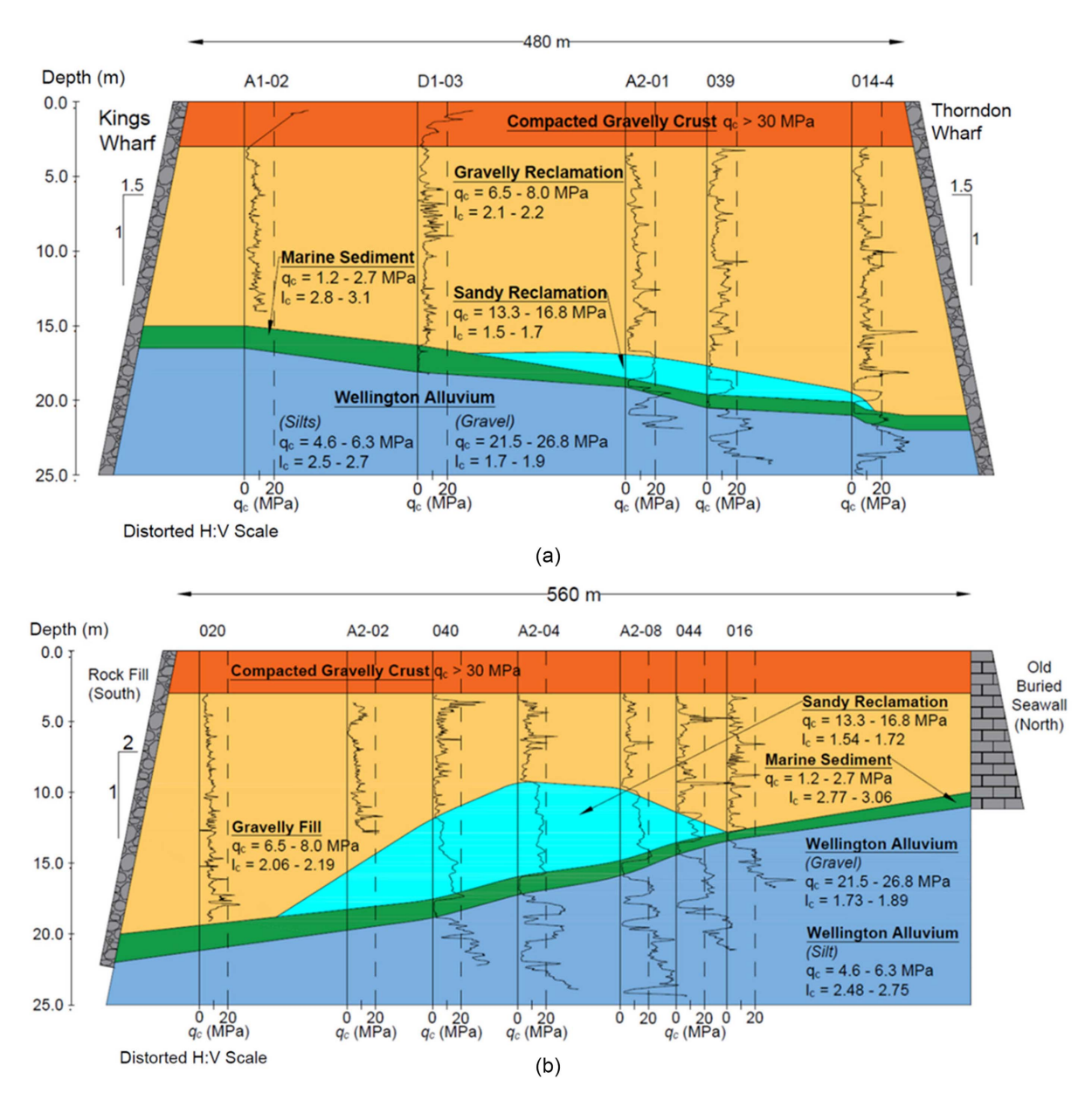


Fig. 3. Subsurface soil profile of Thorndon reclamation from the (a) West-East (W-E); and (b) South-North (S-N) cross-sectional view as characterized by CPTs. (Adapted from Dhakal et al. 2020b.)

soils including some cobble size particles and some fraction of sand and silt (Cubrinovski et al. 2017). A substantial amount of ejecta was typically found near the joints and cracks in the pavement surface, which allowed the liquefied soils to reach the ground surface. Large vertical offsets were observed ranging from tens of centimeters to about 0.5 m among pile-supported wharves, buildings, and the surrounding ground.

Besides the typical ground distress resulting from liquefaction, a global deformation pattern was apparent due to the seaward movement of the reclamation slopes in all unconfined directions, with characteristic liquefaction-induced lateral spread cracks and progressive damage of the ground. As per Dhakal et al. (2020a), liquefaction-induced lateral spread produced lateral displacements of 0.8–1 m near free-faces adjacent to the port and vertical ground settlement of 30–60 cm across the Thorndon reclamation area. Fig. 5 depicts the distribution of observed ejecta, location of ground cracks, and vertical offsets produced at the Thorndon reclamation. A more detailed description of the damage to the land

and structures due to the liquefaction that occurred during the 2016 Kaikōura earthquake has been given by Cubrinovski et al. (2017, 2018).

The Cook Strait event in 2013 produced minor damage over most of the port area except some localized severe damage and partial collapse near the southern edge of the Thorndon reclamation. Lateral displacement of approximately 250 mm along the western edge and 100 mm along the southern edge of the reclaimed land was reported after the Cook Strait event along with some visible cracks and fissures on the surface (Dhakal et al. 2020b; Van Dissen et al. 2013). The Cook Strait event also produced sandy liquefaction ejecta at four locations, but no significant trace of gravelly ejecta was found. On the other hand, the Lake Grasmere event did not produce any direct sign of liquefaction in terms of soil ejecta or any significant damage due to lateral spreading or vertical settlement except relatively negligible wharf damage and ground deformation (Tonkin & Taylor 2014).

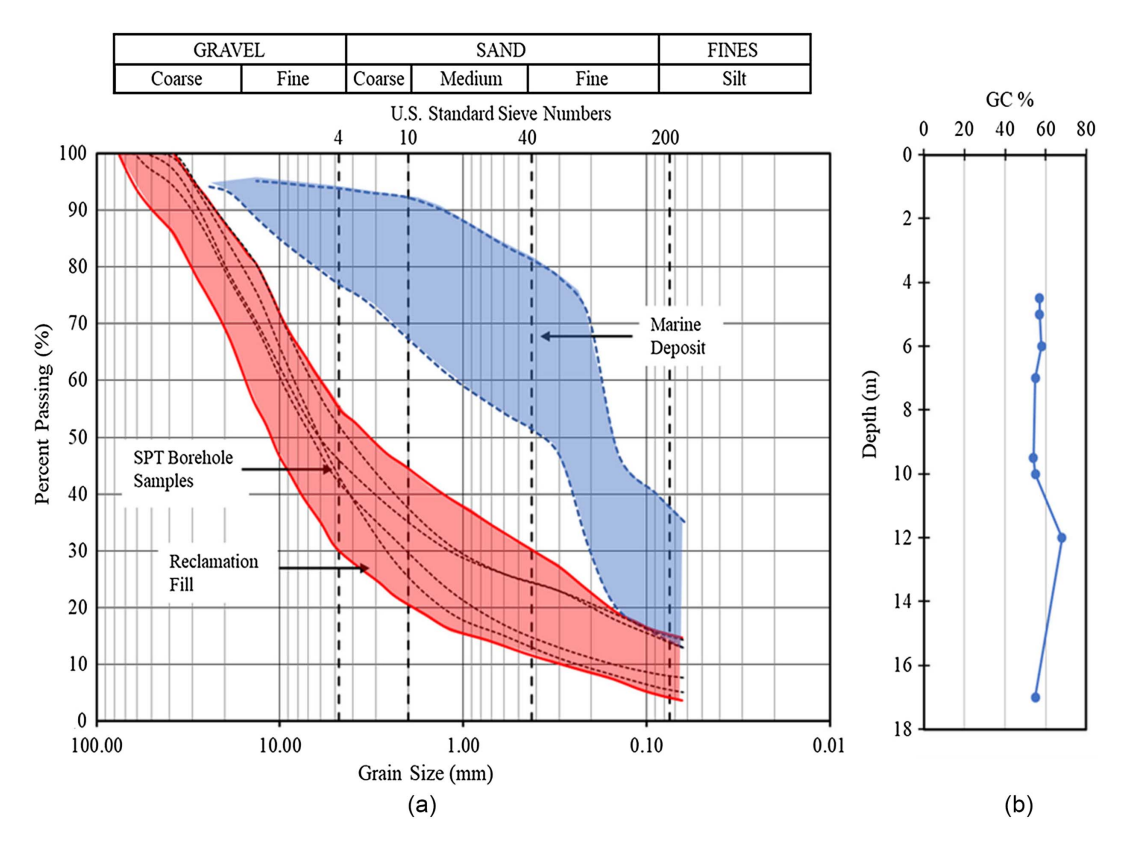


Fig. 4. (a) Particle-size distribution curves for reclamation fill (including SPT samples data) and marine deposits at Centerport (data from Dhakal et al. 2020b); and (b) variation of average gravel content along depth for the reclamation fill deposit based on SPT sampling.

In Situ Testing for Liquefaction Assessment at Centerport

CPT Program

Previous geotechnical testing at Centerport included 121 CPTs to characterize the soil in the reclaimed area of the port, which started in 2017 (Cubrinovski et al. 2018; Dhakal et al. 2020a, b). The CPTs were performed with 10- and 15-cm² A. P. van den Berg I-cones (Heerenveen, Netherlands). The cone soundings were performed using a 218 Geomil Panther 100 rig (Geomil Equipment B. V, Moordrecht, Netherlands) with a push force of 106 kN. Field operations involved predrilling a hole to a depth of approximately 3 m through the asphalt pavement and dense compacted gravelly fill crust that could not be penetrated with the cone. To create the hole, a plugged small-diameter casing with an extractable tip was vibrated slightly beyond the depth at which the penetration rate decreased substantially. The casing had an inside diameter of 55 mm and an outside diameter of 70 mm. This method of predrilling was able to penetrate through the asphalt pavement and concrete (with an open-ended barrel), produced little spoils, and provided lateral support to the CPT rods.

If early refusal was encountered during any test at depths less than approximately 10 m, the cone was pulled up and drilling was performed with a CPT casing beyond the point of refusal until the soil became looser, leaving a cased hole (Bray et al. 2014). Then, the CPT rig was brought into position, pushed to the bottom of the casing, and penetration was resumed to continue further downward. However, the majority of the 75 CPTs in the Thorndon reclamation reached the alluvium. Out of 75 CPTs, there were 17 cases (23%) where refusal was encountered, and it was necessary to predrill to allow further penetration of the CPT. This predrilling approach left a section of the profile (typically a few tens of centimeters) for

which no data were collected. Despite the predrilling efforts, approximately four CPTs could typically be performed in a day, or a little more than 50 m per day by using one CPT rig.

The CPT profiles provide the cone penetration resistance (q_c) and sleeve friction (f_s) versus depth. Based on these q_c and f_s values, the soil behavior type (SBT) index (I_c) was obtained using the following equations proposed by Robertson and Wride (1998):

$$I_c = \{ [3.47 - \log(Q_{tn})]^2 + [1.22 + \log(F_r)]^2 \}^{0.5}$$
 (1)

where Q and F = normalized tip and sleeve friction ratios computed using

$$Q_{tn} = \left(\frac{q_c - \sigma_{vc}}{P_a}\right) \left(\frac{P_a}{\sigma_v'}\right)^n \tag{2}$$

$$F_r = \left(\frac{f_s}{q_c - \sigma_v}\right) \cdot 100\% \tag{3}$$

The Q_{tn} and F_r values within the gravelly fill materials at the six CPTs have been plotted relative to the soil behavior type (SBTn) charts in Fig. 6. When plotting these data, all the layers having $I_c > 2.6$ have been eliminated because those layers can be considered as nonliquefiable. Even though these deposits contained between 45% and 70% gravel, the data points fall into the zones for sands, sandy mixtures, and silt mixtures except for a few points along the border between the sand and gravelly sand zone. Hence, the SBT chart clearly indicates that the behavior of the fill material is governed by the sand and silt fraction, although there is significant amount of gravel content in the soil matrix as found by the sieve analysis based on previously conducted SPT sampling. Although the sandy gravel fill deposits were simply end-dumped and uncompacted so that they would be expected to be normally

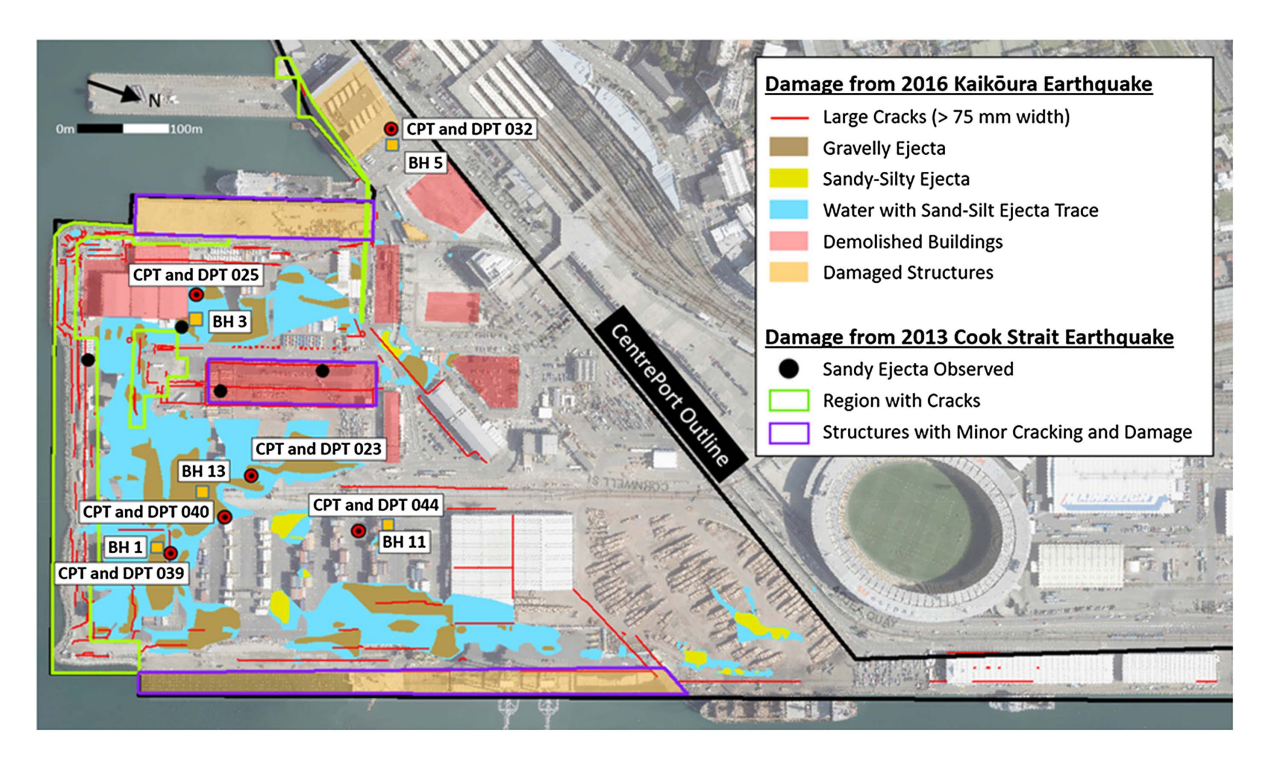


Fig. 5. Map showing the liquefaction ejecta of gravelly and sandy soils along with the manifestation of ground cracks and the damage to structures that occurred during the 2016 Kaikōura earthquake and the 2013 Cook Strait and Lake Grassmere earthquakes. (Adapted from Dhakal et al. 2020a.)

Table 1. Summary of the earthquake events

Earthquake details	$R_{\rm RUP}$ (km)	M_w	PGA (g)
2013 Cook Strait	44	6.6	0.22
2013 Lake Grassmere	65	6.6	0.15
2016 Kaikōura	60	7.8	0.25

consolidated, a significant percentage of the data points were plotted above the normally consolidated wedge as shown in Fig. 6. Overconsolidation could be produced by loading and unloading of cargo container stacks having applied pressures as high as 40 kPa.

In addition, the raw CPT resistance (q_c) was further corrected for the overburden pressure (σ'_v) to obtain q_{c1} profile by using the Boulanger and Idriss (2014) procedure. It should be noted that q_{c1} is a function of equivalent clean sand resistance (q_{c1Ncs}) , which depends on the fines content (FC) of the soil matrix (Boulanger and Idriss 2014). The grain-size distribution of the end-dumped gravelly soil and the ejected samples show a relatively narrow range of fines contents between 5% and 20%. In the present study, a representative FC value of 15% has been used to obtain the equivalent clean sand penetration resistance (q_{c1Ncs}) , consistent with previous studies (Dhakal et al. 2020a, b). The effect of variations in the definition of FC is not considered in this paper.

The CPT results including the profiles of cone penetration resistance (q_{c1}) and SBT index (I_c) are plotted in Figs. 7–12 along with the respective soil profiles of each borehole obtained from the nearby SPT sampling data. It shows that the average q_{c1} for the gravelly reclamation fill based on the six investigated boreholes varies between 8.2 and 9.7 MPa $(q_c$ varying between 5.75 and 8.14 MPa) indicating relatively low average tip resistance which is more or less consistent with the variation of 25th and 75th percentile of q_c between 6.5 and 8.0 MPa as reported by Dhakal et al. (2020a) for all CPT soundings. The value of I_c of the reclamation

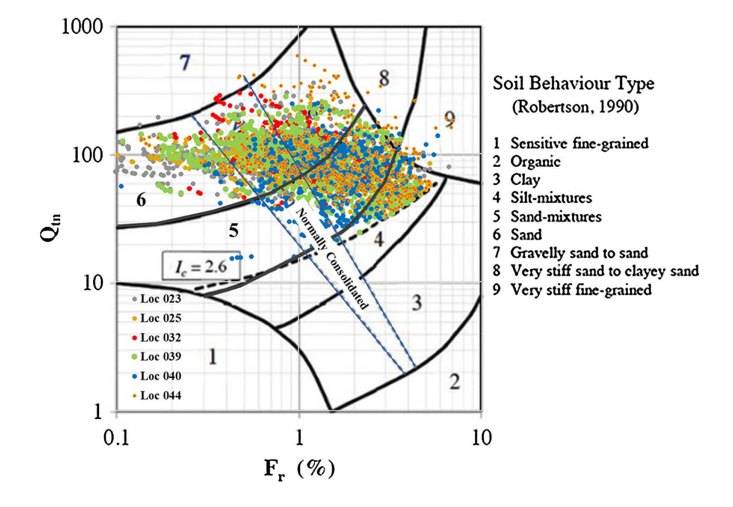


Fig. 6. Distribution of SBT index (I_c) for the reclamation fill deposit for all six boreholes along with the Robertson SBT chart.

fill obtained from these boreholes varies between the range of 1.25–3.98 (average I_c of 1.87–2.26) which is also close to the variation of 25th and 75th percentile of I_c between 2.1 and 2.2, reported by Dhakal et al. (2020a) for all CPT soundings.

Relatively high values of I_c imply that the behavior of the gravelly reclamation fill, consisting of gravel-sand-silt mixtures, would be primarily governed by the silt and sand content despite consisting of 45% to 70% gravel. This fact is also indicated by the SBT chart shown in Fig. 6. The CPT trace distinctly picks up the changes in the main soil layers from gravelly deposits to silty sand reclamation, marine sediment, and Wellington alluvium. The gravelly deposits are 10–14 m thick at Sites 023, 025, 040, and 044; at the other locations (032 and 039), the gravelly deposits are 3–6 m

thick and are underlain by shallow nonliquefiable soil ($I_c > 2.6$) which may either be shallow marine sediments or layers of silty fill (Dhakal et al. 2020b). Below the silty fill, there is a layer of gravelly sand, which may be Wellington Alluvium or a 4-m-thick layer of reclaimed fill (Dhakal et al. 2020b).

DPT Program

As a part of this study, DPT soundings were performed at six locations in the Thorndon reclamation (Locations 023, 025, 039, 040, and 044) and older gravelly reclamations (Location 032) as shown in Fig. 5. As Fig. 5 depicts, the DPT holes are typically located in or near areas where liquefied gravelly soils were ejected during the Kaikōura earthquake. Besides, these DPT holes are also adjacent to the respective CPT holes (within 2–5 m), which were explored by Dhakal et al. (2020a, b) as described in the previous section of the CPT program. Although every DPT hole could not be located in the middle of the observed gravelly ejecta due to some restrictions of local port authority, it does not necessarily indicate that the gravelly soil matrix in those areas did not liquefy, or liquefaction occurred only in sand layer. The manifestation of gravelly or sandy ejecta depends on several factors, e.g., size of soil particles, crack width, flow velocity, and so on.

Sometimes, relatively large particles may not come out on the ground surface due to the self-weight or being obstructed by relatively thin ground fissures (Cao et al. 2011, 2013). Furthermore, most of the port is covered by concrete pavement slabs so that ejecta typically only erupted from joints between panels or cracks. Hence, a certain degree of variability in the ejected materials might be there due to the variation in preferential flow paths at different locations even if the whole soil strata liquefied.

The typical Chinese DPT (Cao et al. 2013) provides a nearly continuous record of the blow count, N_{120} , which represents the

number of hammer blows to drive the penetrometer through a 30-cm interval with a 120-kg hammer dropped from a height of 1 m. To provide increased resolution, raw blow counts are typically reported at every 10 cm of penetration but are multiplied by three to get the equivalent N_{120} for 30 cm of penetration. In this study, the DPT tests were conducted using a drill rig having an SPT safety hammer with a weight of 63.5 kg dropped from a height of 0.76 m. The energy transferred to the drill rods by the SPT hammer was measured using a pile driving analyzer (PDA). These measurements indicated that the SPT hammer delivered an average of 83.5% of the theoretical SPT free-fall energy. Because the energy delivered by the SPT hammer (E_{Hammer}) produced different energy than that supplied by a standard Chinese DPT hammer ($E_{\text{Chinese DPT}}$) (Cao et al. 2011), the measured blow counts were converted to the equivalent Chinese energy standard blow counts (N_{120}) by applying the linear energy correction method of Seed et al. (1985) as given by Eq. (4), which was also reported by Rollins et al. (2021)

$$N_{120} = N_{\text{Hammer}} \left(E_{\text{Hammer}} / E_{\text{Chinese DPT}} \right)$$
 (4)

An average energy ratio was measured in the present study instead of measuring actual energy at different depths of each borehole. Hence, an average energy correction factor was applied to correct measured blow counts along the depth for all the boreholes. These energy corrected N_{120} has been further converted to N_{120}' by applying the Cao et al. (2013) overburden correction procedure as described by Rollins et al. (2021). These corrected N_{120}' profiles for all the boreholes are plotted in Figs. 7–12 next to the plots of CPT resistance (q_{c1} and I_c) for a direct comparison between the results of DPT and CPT. The DPT penetration resistance (N_{120}') for all the locations was consistently around or below 10 on average except at Location 032, potentially due to the presence of silty fill and dense gravelly sand reclamation strata as interpreted by the CPT.

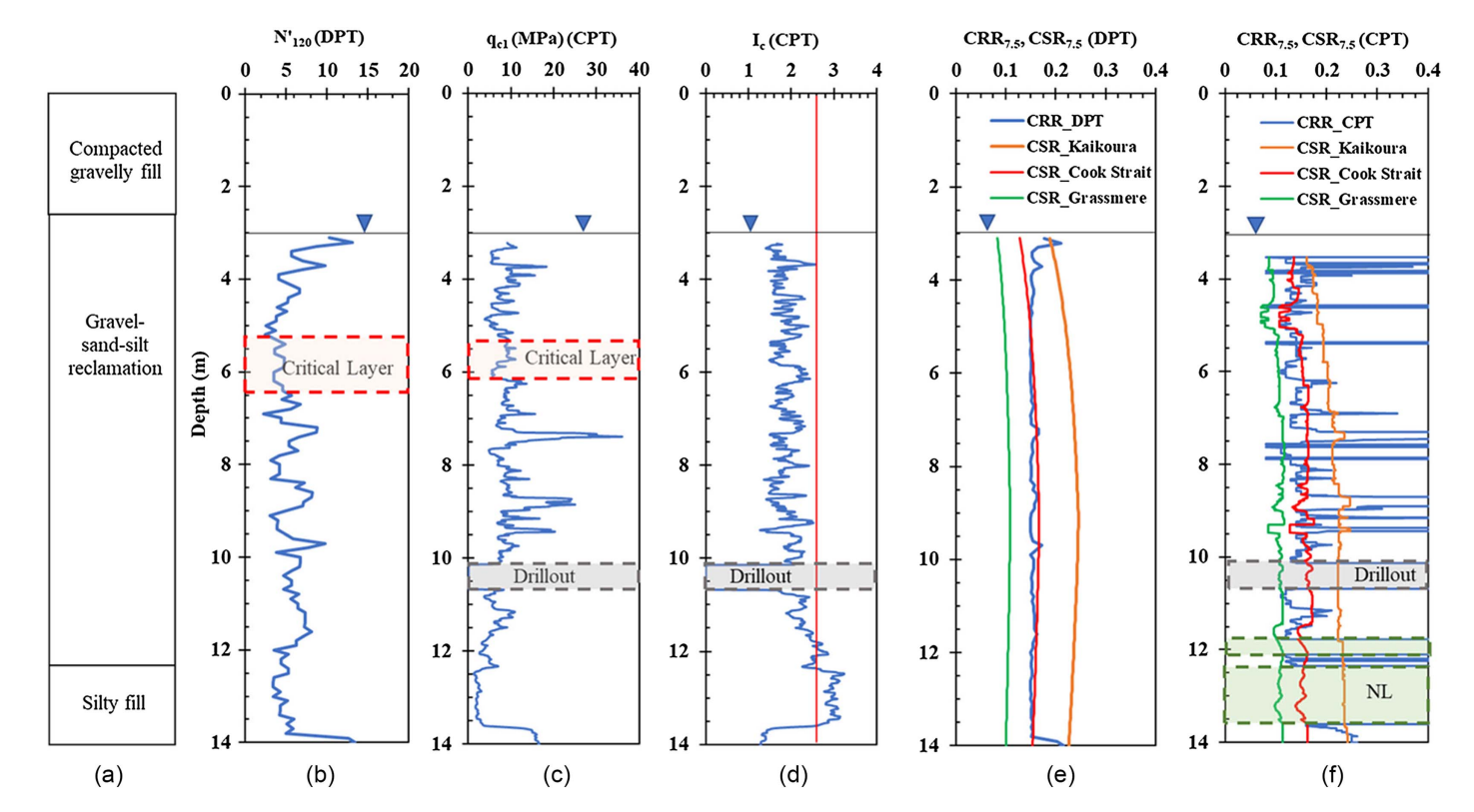


Fig. 7. Profiles indicating (a) soil profile; (b) DPT blow count, N'_{120} ; (c) CPT cone resistance, q_{c1} ; (d) soil behavior type, I_c ; (e) CRR and CSR from DPT; and (f) CSR and CRR from CPT for Location 023. Nonliquefiable (NL) layers are shown by shaded rectangles in plot (f).

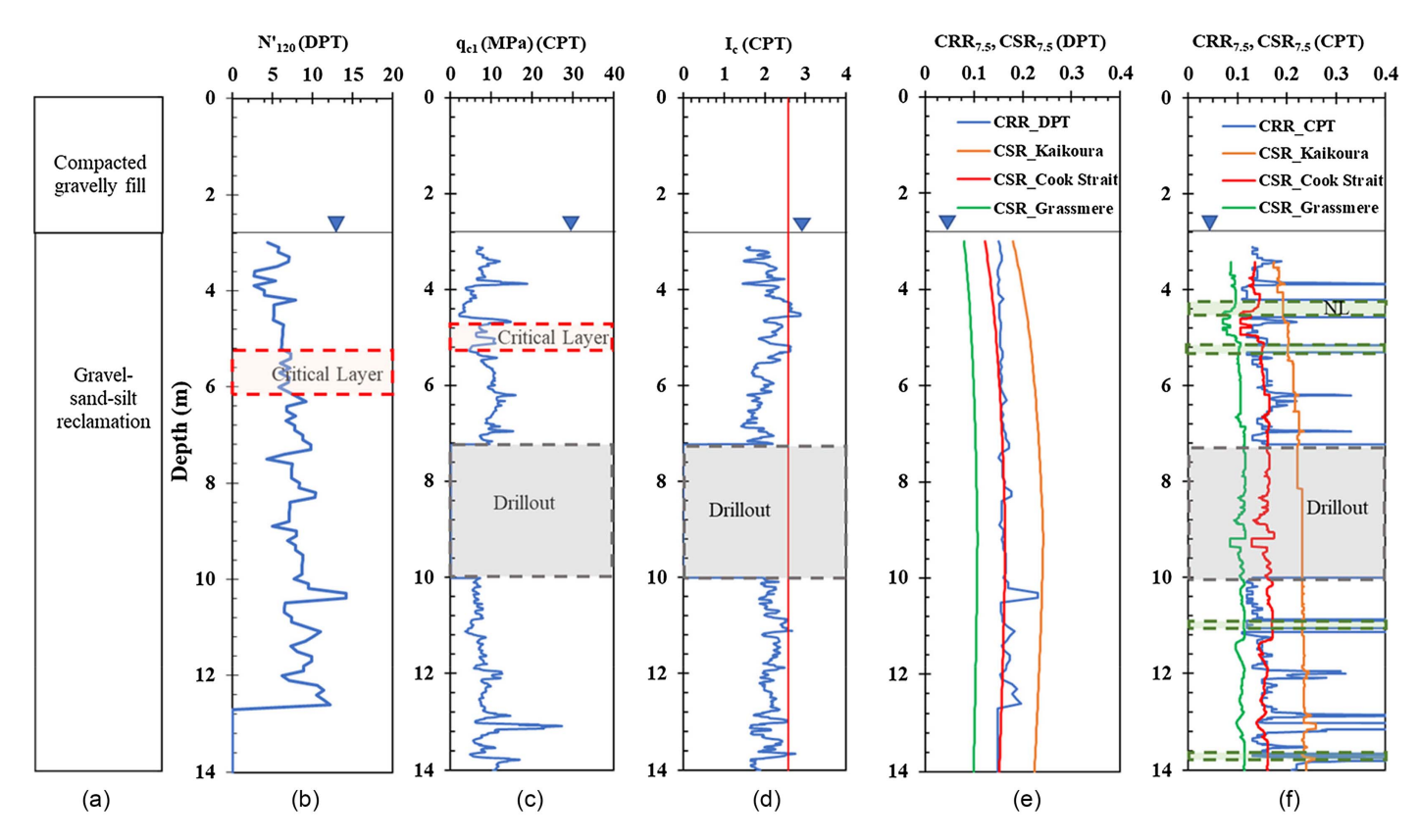


Fig. 8. Profiles indicating (a) soil profile; (b) DPT blow count, N'_{120} ; (c) CPT cone resistance, q_{c1} ; (d) soil behavior type, I_c ; (e) CRR and CSR from DPT; and (f) CSR and CRR from CPT for Location 025. NL layers are shown by shaded rectangles in plot (f).

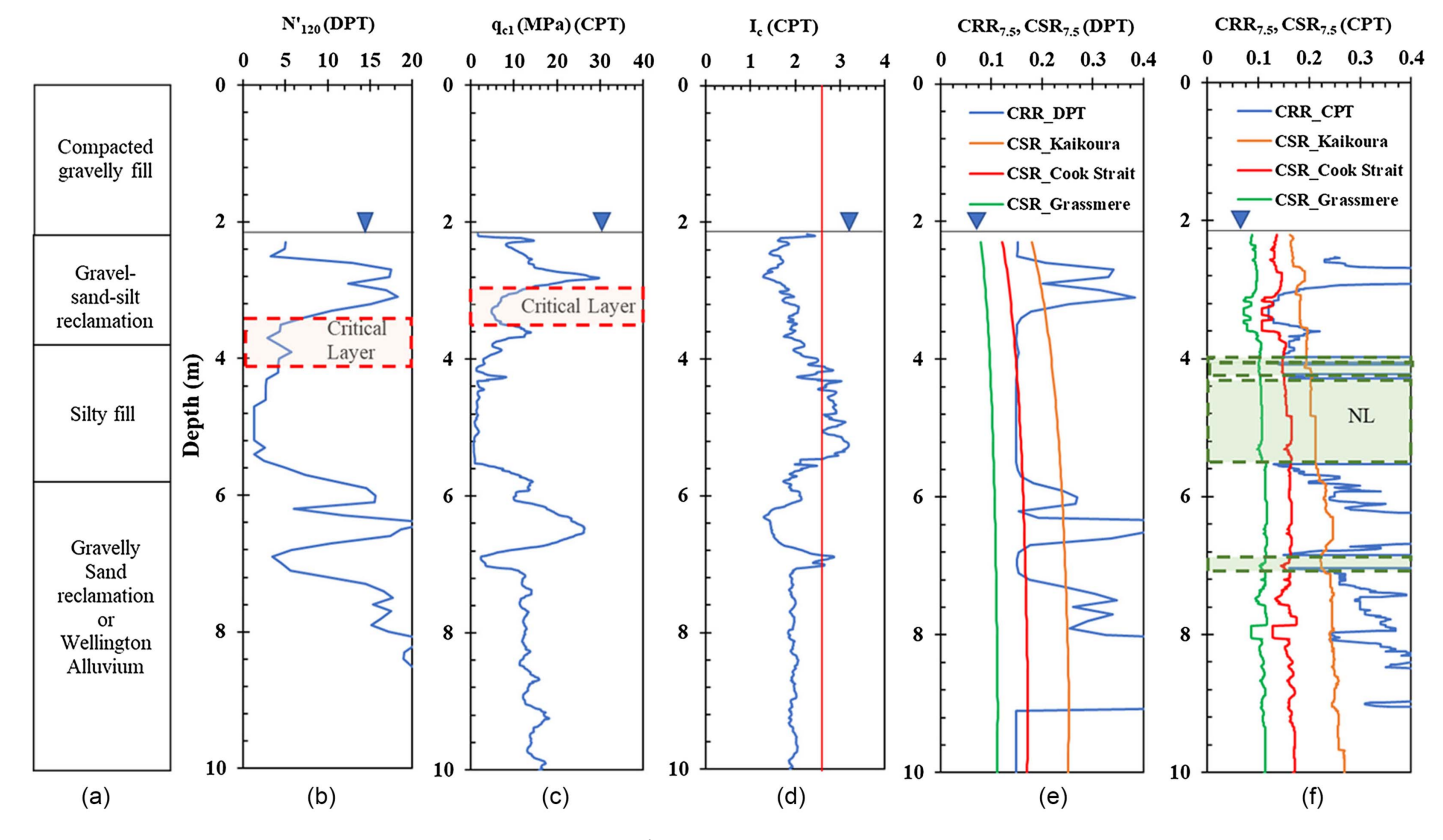


Fig. 9. Profiles indicating (a) soil profile; (b) DPT blow count, N'_{120} ; (c) CPT cone resistance, q_{c1} ; (d) soil behavior type, I_c ; (e) CRR and CSR from DPT; and (f) CSR and CRR from CPT for Location 032. NL layers are shown by shaded rectangles in plot (f).

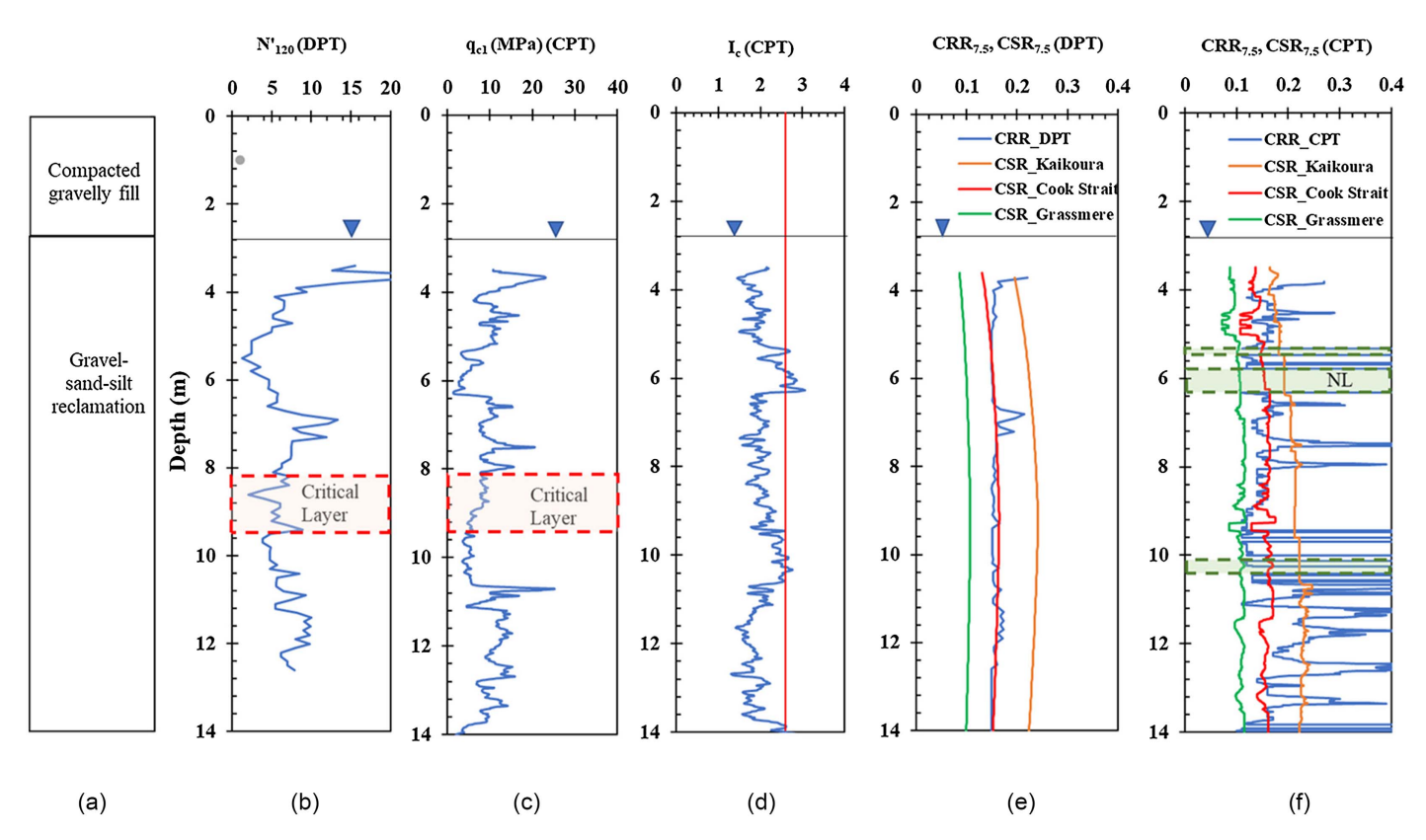


Fig. 10. Profiles indicating (a) soil profile; (b) DPT blow count, N'_{120} ; (c) CPT cone resistance, q_{c1} ; (d) soil behavior type, I_c ; (e) CRR and CSR from DPT; and (f) CSR and CRR from CPT for Location 039. NL layers are shown by shaded rectangles in plot (f).

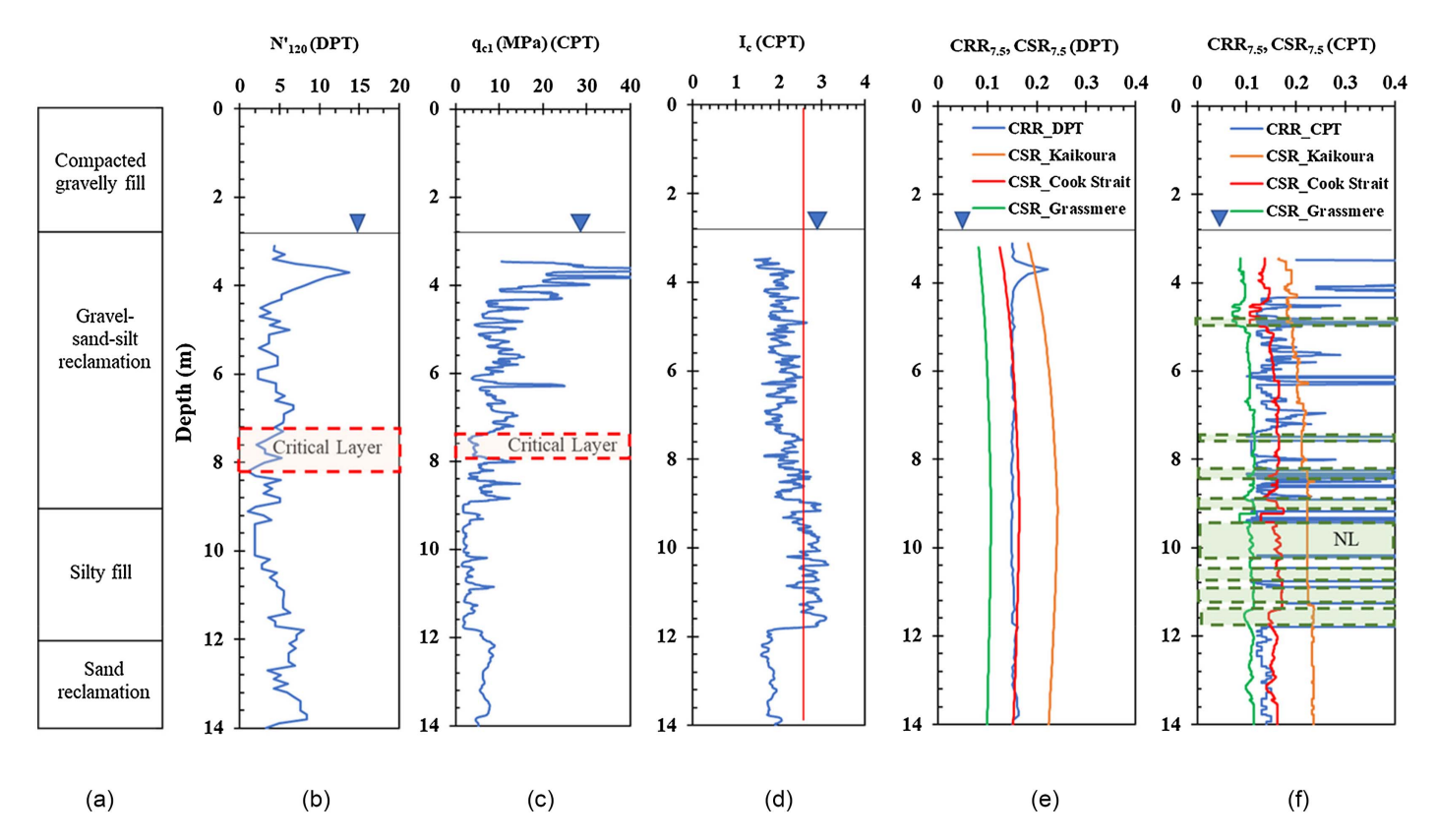


Fig. 11. Profiles indicating (a) soil profile; (b) DPT blow count, N'_{120} ; (c) CPT cone resistance, q_{c1} ; (d) soil behavior type, I_c ; (e) CRR and CSR from DPT; and (f) CSR and CRR from CPT for Location 040. NL layers are shown by shaded rectangles in plot (f).

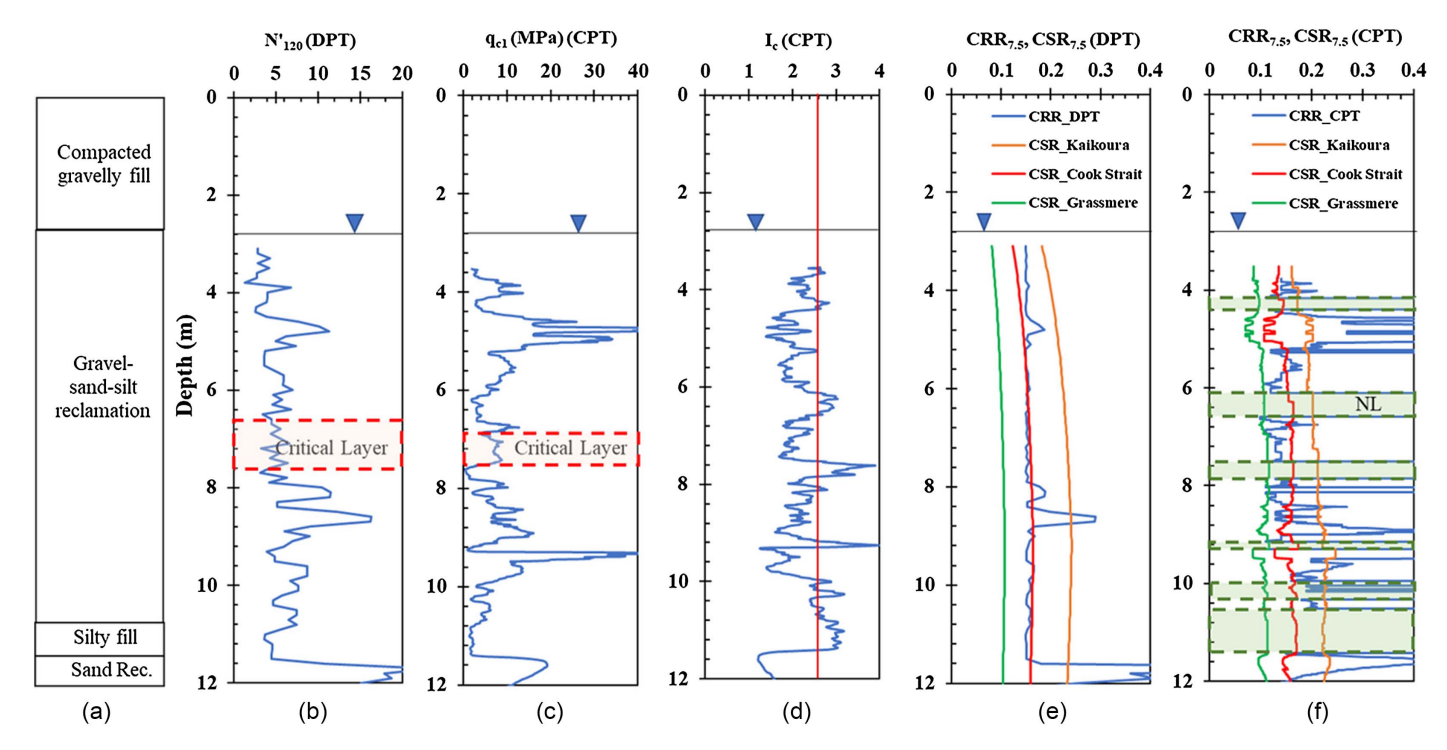


Fig. 12. Profiles indicating (a) soil profile; (b) DPT blow count, N'_{120} ; (c) CPT cone resistance, q_{c1} ; (d) soil behavior type, I_c ; (e) CRR and CSR from DPT; and (f) CSR and CRR from CPT for Location 044. NL layers are shown by shaded rectangles in plot (f).

Comparison between the Results of the CPT and DPT

Comparing the N'_{120} and q_{c1} profiles side by side, it can be observed that the N'_{120} profile is considerably smoother and more uniform for most of the locations in contrast to the q_{c1} profile, which has several intermittent spikes along its depth. Although the CPT response (q_{c1} and I_c values) indicates that the behavior of the reclamation fill is dominated mostly by the finer fractions, a considerable amount of gravel particles (about 45% to 70%) still remain in the soil matrix (Cubrinovski et al. 2017). Therefore, it seems likely that these gravel particles might have had a more significant effect on the small-diameter CPT cone resistance compared with the larger diameter DPT cone. This phenomenon would explain the high q_{c1} values at various depths along the gravelly deposit in the CPT profile that are not present in the DPT profile.

In Figs. 6 and 7, there are two locations where there is an interruption in the CPT q_{c1} profile. Gaps (drill-out zones) exist from 10.1 to 10.7 m for Location 023 and from 7.2 to 10 m in Location 025. These are locations where the CPT reached early refusal so it was necessary to drill through the dense layer before resuming the CPT sounding. The DPT was instead able to penetrate these layers and provide a more complete profile.

The DPT is not able to identify the soil types as the CPT does based on the SBT index (I_c) . This is a significant advantage of the CPT because it could obtain more detailed characterization of heterogeneous soil deposits including small variations in I_c often caused due to the presence of thin layers which could not be captured by the DPT. A companion CPT or core hole would be necessary to define nonliquefiable layers for DPT investigations. However, considering the pros and cons of each side, both CPT and DPT together performed reasonably well in obtaining continuous profiles of penetration resistance and characterizing the soil layers in detail at the Port of Wellington.

Liquefaction Evaluation Based on the CPT

Based on the q_{c1} profiles shown in Figs. 7–12, the cyclic resistance ratio (CRR_{M=7.5}) required to cause liquefaction has been obtained versus depth for each test using the Boulanger and Idriss (2014) CPT-based liquefaction triggering procedure. The CRR_{M=7.5} versus depth profiles have been obtained for a 50% probability of liquefaction. Although 15% probability is often recommended for forward design, in this study, the 50% probability curve has been considered to avoid overconservatism in estimating the factor of safety against liquefaction, especially because these estimates are compared with observations.

The cyclic stress ratio (CSR) versus depth profile for each site has been obtained for the three seismic events (2016 Kaikōura and 2013 Cook Strait and Lake Grassmere earthquakes) by using the simplified procedure of Seed and Idriss (1971). To facilitate comparisons between the CRR and CSR profiles, the CSR profiles have been converted to $CSR_{M=7.5}$ for all the earthquake events by using the equation

$$CSR_{M_{o}7.5} = CSR/MSF \tag{5}$$

where MSF = magnitude scale factor obtained by using the equation recommended in the Boulanger and Idriss (2014) CPT-based liquefaction triggering procedure.

Plots of the CRR and CSR versus depth for M_w 7.5 are shown in Figs. 7–12. These plots show that the CRR profiles have formed several intermittent spikes along the depth, potentially due to the effect of CPT probe interaction with gravel particles or due to relatively high I_c values indicating a nonliquefiable soil matrix. However, the average CRR values excluding the occasional spikes mostly remained in the range of 0.1–0.2, which is much less than the CSR for the Kaikōura event. Therefore, liquefaction is estimated to trigger for the Kaikōura event based on the average CPT resistance.

CSRs for the Lake Grassmere event were lower than the average values of CRRs, indicating that liquefaction is not estimated to trigger except for a few very thin layers. Hence, the results for the Lake Grassmere earthquake are relatively consistent with the lack of liquefaction observed. On the other hand, the CSR profile for the Cook Strait event remained just slightly higher than the average values of CRR (excluding the spikes) with liquefaction predicted in relatively thin layers, less than 1 m in thickness, above a depth of 6 m. Therefore, the CRR and CSR plots for the Cook Strait event indicate a marginal chance of liquefaction occurrence within the gravelly layers. This evaluation remains consistent with the occurrence of localized damage including the lateral spreading and vertical settlement produced along the southern and western edges of the Thorndon reclamation along with limited liquefaction ejecta of sandy soil. Of course, there is also a possibility that liquefaction occurred at greater depths but did not produce any gravel ejecta on the surface.

Triggering Analysis

To evaluate the liquefaction potential of all points together against the set of liquefaction triggering curves of Boulanger and Idriss (2014), the critical layers for each borehole were first identified by using the criterion of lowest average factor of safety, i.e., the layer that produces the lowest average ratio of $CRR_{M=7.5}$ to $CSR_{M=7.5}$. In the case of CPT, the critical layer has been over a thickness of about 0.5 m to represent a consistent q_{c1} resistance

that is less affected by thin peaks and troughs (Boulanger and Idriss 2014). Also, the critical layer has been identified at the shallower depth below the GWT because that layer would be the most likely to trigger and manifest liquefaction at the ground surface (Green et al. 2014; Dhakal et al. 2020b).

The location and the thickness of representative critical layers for all the boreholes are depicted by the dashed lines in Figs. 6–11. Layers with I_c values higher than 2.6 were screened out as claylike soil layers that are considered nonliquefiable (Boulanger and Idriss 2014). The boundary line for $I_c=2.6$ is shown by solid vertical lines on the plots of I_c , and the layers with I_c greater than 2.6 have been marked with shaded zones on the CRR plots in Figs. 7–12 to indicate the nonliquefiable (NL) layers. In addition, thin interbedded layers with high q_{c1} peaks, which can be caused by the interaction with large gravel particles, have also been excluded in calculating the average penetration resistance of the selected critical layers.

Based on the representative critical layer at each borehole, the average equivalent clean sand penetration resistance (q_{c1Ncs}) and CSR were obtained for all the earthquake events. The pairs of q_{c1Ncs} and CSR have then been plotted as liquefaction or no-liquefaction data points along with the CPT-based triggering curves as shown in Fig. 13. The results indicate that the (CSR, q_{c1Ncs}) data points corresponding to the Kaikōura event, which produced widespread liquefaction manifestation on the ground surface, fell well above the 85% triggering line and hence the estimation of liquefaction triggering was consistent with the actual case history.

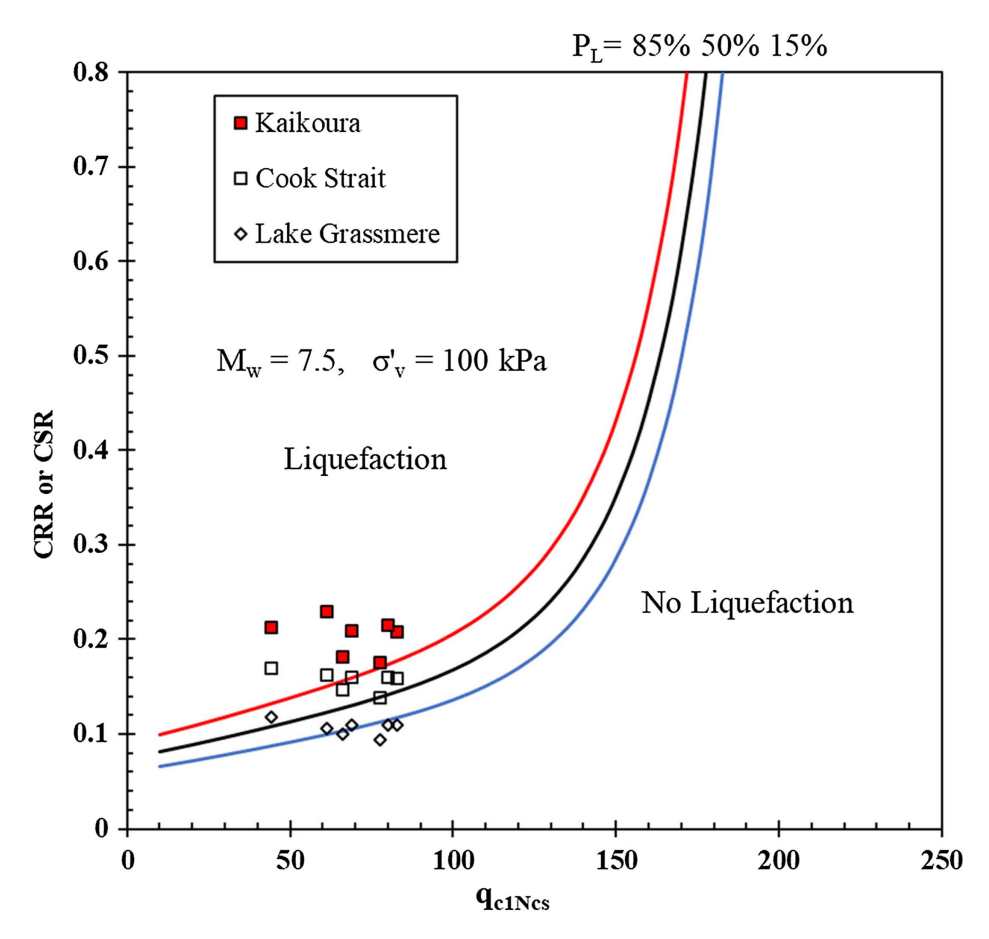


Fig. 13. Comparison of average CSR- q_{c1Ncs} points in the critical zone for CPT holes for three earthquakes at Wellington Port in comparison with CPT-based probabilistic liquefaction triggering curves. Solid markers indicate liquefaction sites and open markers indicate no liquefaction. (Data from Boulanger and Idriss 2014).

The points for the Lake Grassmere event fell below the 50% triggering line, indicating very little chance of triggering liquefaction, which is more or less consistent with the real case history because there was no significant damage or liquefaction ejecta observed after this earthquake except some minor cracking at a few locations.

For the Cook Strait event, most of the points fell above the 50% but below the 85% triggering curve, suggesting a moderate chance of liquefaction. This slightly overestimated the actual event, which produced some localized manifestation near the Thorndon extension along with some sandy ejecta but not as severe as the Kaikōura event that produced extensive liquefaction manifestation throughout the reclamation fill. Besides, near the boreholes considered in the present study, no indication of gravel ejecta was observed after the Cook Strait event. However, plotting results from the critical layers only can be somewhat deceptive because this approach does not consider the liquefaction potential of the entire profile, which was characterized by thin layers of liquefaction, as discussed previously.

Overall, the CPT-based liquefaction triggering procedure of Boulanger and Idriss (2014) performed well for very low and medium-to-high seismic demands of the Lake Grassmere and Kaikōura earthquakes, respectively, but the performance remained marginal near the threshold of liquefaction triggering for the seismic demand induced by the Cook Strait earthquake (Dhakal et al. 2020b). The probable reason behind this fact can be that small uncertainties in the seismic demand, fines content, or other factors associated with using the simplified procedure can lead to important variations in the potential for liquefaction when the CSR is close to the CRR.

Liquefaction Evaluation Based on the DPT

Based on the DPT N_{120}' profiles shown in Figs. 6–11, the CRR versus depth profiles have been obtained for all the boreholes using the DPT-based liquefaction triggering procedure of Rollins et al. (2021) for 50% probability of liquefaction ($P_L=0.5$) corresponding to M_w 7.5. This is the same probability as used in the CPT assessment. In addition, CSR profiles have been obtained by using the simplified procedure of Seed and Idriss (1971) as described in the section on CPT. To further facilitate comparison between the CRR and CSR profiles for every site, the CSR profiles have been converted to the reference magnitude of M_w 7.5 by using the DPT-based MSF given by Rollins et al. (2021).

The computed $CRR_{M=7.5}$ and $CSR_{M=7.5}$ profiles for the three different earthquake events (Kaikōura, Cook Strait, and Lake Grassmere) at the port are plotted together in Figs. 6–11 for all the DPT boreholes. These plots show that the CSR values for the Kaikōura event are considerably higher than CRR, therefore estimating a low factor of safety for liquefaction triggering throughout the depth of the gravelly deposits. These results are consistent with the observations of large volumes of gravelly soil ejecta erupting at the ground surface.

In contrast, the CSR versus depth profiles for the Lake Grassmere event remain lower than the CRR profiles, indicating higher factors of safety against liquefaction or lower probabilities of liquefaction. This is consistent with the actual scenario for the Lake Grassmere event, which hardly produced any liquefaction manifestation on the surface. For the Cook Strait event, the CRR curve versus depth was generally similar to the CSR curves, with some layers having CRR values slightly higher, and for some parts of the fill, the CRR was slightly lower than CSR, indicating a marginal chance of liquefaction. This result is consistent with some observed features of localized damages at the port, including lateral spreading and liquefaction ejecta near the Thorndon extension.

But liquefaction manifestations were not as extensive around the whole reclamation site, as occurred during the Kaikōura event.

Triggering Analysis

To provide a summary of the liquefaction potential for all sites, a simplified triggering analysis has been performed by using the newly developed DPT-based triggering curves of Rollins et al. (2021). To perform the triggering analysis, the critical layer has first been selected for every test hole following the similar procedure described for the CPT-based triggering analysis, i.e., by subjectively considering the effect of depth, thickness, and the factor of safety in a holistic manner to select the potential layer most likely to produce liquefaction manifestation on the ground surface. In the case of the DPT, both N'_{120} and CRR profiles were relatively consistent and do not reflect significant variation in the liquefaction resistance for thin interbedded layers, unlike the CPT. Therefore, the critical layers for the DPT have typically been selected over an interval of 1 m or more to provide a more representative N'_{120} avoiding the effects of thin peaks and troughs existing in the DPT profiles.

Like the CPT, several layers with low N_{120}' values, but having I_c greater than 2.6, have been excluded from consideration as the critical layer because $I_c > 2.6$ from the CPT implies that the soils are not susceptible to liquefaction. The location and the thickness of the critical layers for all the DPT profiles are depicted by the dashed lines in Figs. 6–12.

Based on the identified critical layers, the average CSR and N'_{120} has been obtained for each borehole. These pairs of CSR and N'_{120} have then been plotted for all three earthquakes in Fig. 14 along with the DPT-based triggering curves to facilitate comparisons with the 50% triggering line. Fig. 13 shows that the liquefaction points corresponding to the 2016 Kaikōura event fell well above the 85% triggering line, indicating a high chance of liquefaction occurrence, which is consistent with the widespread liquefaction manifestation that occurred after the event. On the other hand, the points of no-liquefaction corresponding to the 2013 Lake Grassmere event fell much below the 50% triggering line, indicating almost no chance of triggering liquefaction, which is also consistent with the actual case history where hardly any liquefaction manifestation (a few minor cracks but no ejecta or significant damage) occurred after this event.

The points corresponding to the Cook Strait event fell just below the 50% line, indicating a marginal chance of liquefaction occurrence, which is also consistent with the localized lateral spreading and corresponding damage near the Thorndon extension, although the entire reclaimed area was not severely damaged as during the Kaikōura event. Hence, the DPT-based liquefaction triggering procedure was generally successful in evaluating the liquefaction potential of the Thorndon gravelly reclamation for all three earthquake events. Nevertheless, a certain degree of uncertainty is inherent in the DPT-triggering method because it does not account the effect of fines content in estimating the liquefaction triggering potential.

Comparison between the Liquefaction Evaluation Based on CPT and DPT

To draw a comparison between the liquefaction evaluation based on the CPT and DPT, the CRR profiles obtained from both tests are plotted together in Fig. 15 for all the sites. Fig. 14 shows that the DPT-based CRR profiles were closely aligned with the average CPT-based CRR profiles excluding the occasional spikes. However, the intermittent spikes observed in the CPT-based CRR

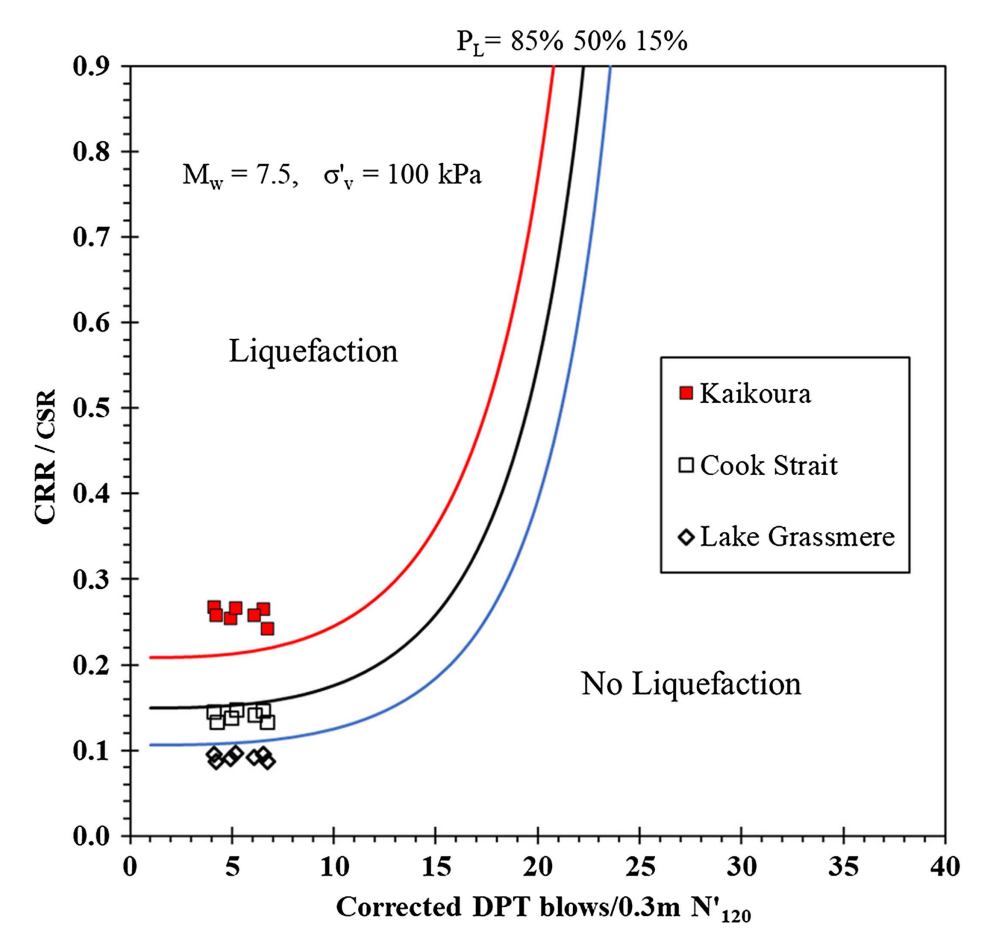


Fig. 14. Comparison of average $CSR-N'_{120}$ points in the critical zone for DPT holes for three earthquakes at Centerport in comparison with DPT-based probabilistic liquefaction triggering curves (data from Rollins et al. 2021). Solid markers indicate liquefaction sites, and open markers indicate no liquefaction.

profiles were absent in the DPT-based CRR profiles. This inconsistency between the DPT and CPT results can be explained by the concept of particle-size effect on the penetrometers used in the respective in situ tests. The particle-size distribution shown in Fig. 4 indicates that the gravel content for the Thorndon reclamation fill was about 60%–70%. The average particle size, D_{50} , for most of the samples was around 6 to 7 mm. However, about 30% to 40% of the gravel particles were in the range of 10 to 15 mm. Hence in the case of the DPT, the cone with a diameter of 74 mm and a cone angle of 60° can easily penetrate these larger gravel particles without any artificial increase in resistance from large particle—cone interaction. Therefore, the DPT did not produce intermittent spikes in the N'_{120} or CRR profiles at the port of Wellington, despite the presence of gravel particles in the soil layers.

In the case of the CPT, the diameters of the 10- and 15-cm² cones were 18 and 22 mm. Therefore, the gravel particles with diameters of 10 to 15 mm may obstruct the penetration of the CPT probe, yielding some occasional spikes in the penetration resistance q_c and the corresponding CRR profiles. However, because the gravelly deposit of the reclamations is primarily governed by the sand and silt content, which is indicated by the average q_c of 5.75–8.14 MPa and I_c of 1.87–2.26 [with the 25th and 75th percentiles of q_c and I_c lying between 6.5 and 8 MPa and 2.1–2.2, respectively, as per Dhakal et al. (2020a)], the overall liquefaction potential of the fill deposit was not affected by the occasional spikes, and the average CPT-based CRR profile was in good agreement with the DPT-based CRR profiles. This fact is also consistent with the results of Roy and Rollins (2022), which showed that the pore pressure

generation in gravelly soil is governed by the hydraulic conductivity of the soil matrix, which in turn is significantly controlled by the amount of sand and silt content remaining in the soil matrix. Roy and Rollins (2022) reported a large amount of gravel liquefaction case history data where the variation of sand content was found to be 20% to 90% in the liquefiable gravelly deposits.

On the other hand, the CPT could capture the subtle changes in penetration resistance caused by the thin seams of nonliquefiable soil. These thin interbedded layers are reflected by the off-scale spikes on the CRR profiles formed at the locations where I_c was greater than 2.6. These portions have been carefully excluded when analyzing the particle-size effect by using the $I_c=2.6$ line, which clearly discriminates the nonliquefiable clayey layers ($I_c>2.6$) shown by shaded layers on the CRR plots in Figs. 7–12. Therefore, in terms of liquefaction assessment, the high sensitivity of the CPT to the soil composition and density state of the soil matrix proves to be highly beneficial for identifying thin nonliquefiable interbedded layers.

The triggering analyses performed by both CPT and DPT (Figs. 13 and 14) estimated a high chance of liquefaction occurrence for the Kaikōura event, but almost no chance of liquefaction for the Lake Grassmere event. For the Cook Strait event, both methods estimated a marginal degree of liquefaction, with the CPT indicating probabilities somewhat higher than 50% and the DPT indicating probabilities just below 50%. However, the overall consistency of the estimated degree of liquefaction with the actual case histories for each event confirmed the reliability of both the CPT-and DPT-based triggering procedures for evaluating liquefaction

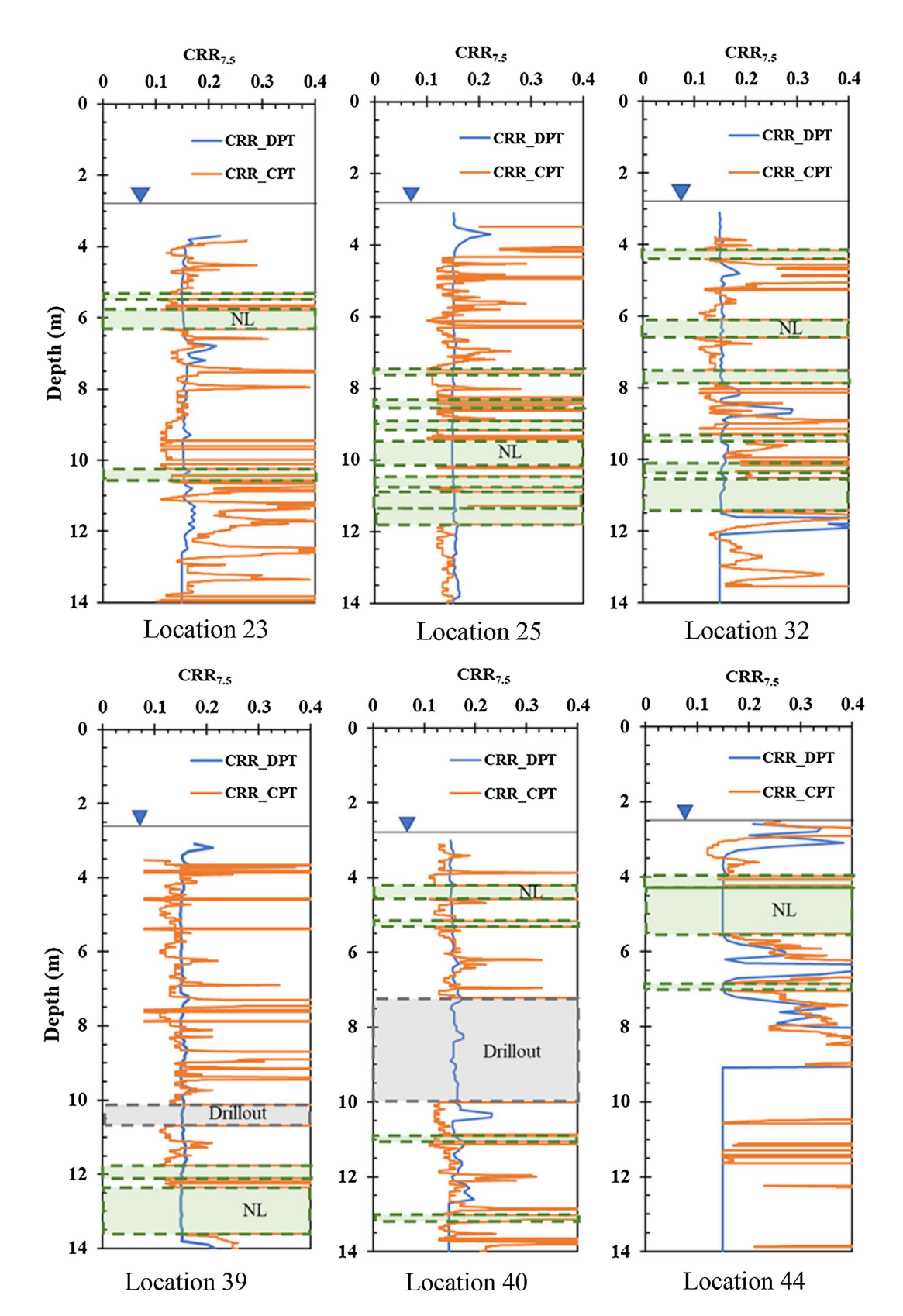


Fig. 15. Comparison of CRR versus depth curves obtained from DPT-based (data from Rollins et al. 2021) and CPT-based (data from Boulanger and Idriss 2014) triggering curves at 50% probability of liquefaction. NL layers shown by shaded rectangles.

potential of the Thorndon reclamation at Centerport. Of course, a certain degree of uncertainty would still be expected for each of these triggering procedures. Considering that both methods were independently developed from separate data sets, the agreement between the two methods confirm the reliability of both methods.

Summary and Conclusions

CPTs and DPTs tests performed at seven locations in the Thorndon reclamation of Centerport at Wellington, New Zealand. These sandy gravel fill deposits liquefied, producing a large volume of sandy gravel ejecta along with significant lateral and vertical displacements during the M_w 7.8. Kaikōura earthquake in 2016. However, marginal liquefaction was observed during the M_w 6.6 Cook Strait earthquake, and almost no liquefaction was found during the M_w 6.6 Lake Grassmere earthquakes in 2013. Based on this comparative study of liquefaction potential using CPT- and DPT-based methods at the port of Wellington, the following conclusions can be drawn:

- The Robertson chart indicates that the SBT of the reclamation fill is primarily governed by the sand and silt content because most points fall in the region of the sand zone, although significant amounts of gravel content remained in the soil matrix.
- The CRR versus depth curves obtained from the DPT were very similar to the average CRR versus depth curves, excluding the occasional spikes from the CPT, which confirms the consistency of both methods in assessing liquefaction resistance in the loose gravel-sand-silt deposits at Centerport, considering that both methods were developed independently.
- Generally, the DPT yielded relatively smooth profiles of low penetration resistance (N'_{120}) , whereas the CPT profiles exhibited occasional spikes in penetration resistance with depth. This implies that the larger-diameter DPT penetrometer was less influenced by gravel-sized particles and obtained more stable resistance relative to the CPT. However, the soil behavior at the Thorndon reclamation is primarily governed by the permeability of thesand and silt content as suggested by average I_c values and hence the occasional spikes in CPT profiles do not alter the prevalent q_c values that govern the outcomes in the liquefaction evaluation.
- Both the CPT- and DPT-based CRR remained consistently lower than the CSR for the Kaikōura event, indicating a high probability of liquefaction, which is consistent with observed liquefaction features. For the Lake Grassmere event, CRRs from the CPT and DPT were consistently higher than the CSR, indicating relatively little chance of liquefaction occurrence, as was observed. For the Cook Strait event, the CRR profiles were typically close to the CSR with depth, indicating a marginal chance of liquefaction manifestation, which is also consistent with the localized damage observed near the southern and western edge of the reclamation site.
- Overall, both triggering procedures satisfactorily evaluated the probability of liquefaction occurrence at the Thorndon reclamation site, although a certain degree of uncertainty exists individually in each procedure, particularly in estimating the probability of liquefaction for marginal events.

Data Availability Statement

Some data, models, or code that support the findings of this study are available from the corresponding author upon reasonable request. These data include electronic versions of DPT profile and DPT-based liquefaction resistance profiles.

Acknowledgments

Funding for this study was provided by Grant G16AP00108 from the USGS Earthquake Hazard Reduction Program and Grant CMMI-1663546 from the National Science Foundation. This funding is gratefully acknowledged. However, the opinions, conclusions, and recommendations in this paper do not necessarily represent those of the sponsors. We also express sincere appreciation to Tiffany Krall and Rick Wentz for arranging access for DPT testing at Centerport in Wellington, New Zealand.

References

- Andrus, R. D. 1994. "In situ characterization of gravelly soils that liquefied in the 1983 Borah Peak earthquake." Ph.D. thesis, Dept. of Civil Engineering, Univ. of Texas at Austin.
- Athanasopoulos-Zekkos, A., D. Zekkos, K. M. Rollins, J. Hubler, J. Higbee, and A. Platis. 2019. "Earthquake performance and characterization of gravel-size earthfills in the ports of Cephalonia, Greece, following the 2014 Earthquakes." In Proc., 7th Intl. Conf. on Earthquake Geotechnical Engineering for Protection and Development of Environment and Constructions, 1212–1219. London: Taylor and Francis.
- Boulanger, R. W., and I. M. Idriss. 2014. CPT and SPT based liquefaction triggering procedures. Rep. No. UCD/CGM-14. Davis, CA: Univ. of California.
- Bradley, B. A., H. N. Razafindrakoto, and V. Polak. 2017. "Ground-motion observations from the 14 November 2016 M_w 7.8 Kaikōura, New Zealand, earthquake and insights from broadband simulations." *Seismol. Res. Lett.* 88 (3): 740–756. https://doi.org/10.1785/02201 60225.
- Bradley, B. A., L. M. Wotherspoon, A. E. Kaiser, B. R. Cox, and S. Jeong. 2018. "Influence of site effects on observed ground motions in the wellington region from the M_w 7.8 Kaikōura, New Zealand Earthquake." Bull. Seismol. Soc. Am. 108 (3B): 1722–1735. https://doi.org/10.1785/0120170286.
- Bray, J. D., J. D. Zupan, M. Cubrinovski, and M. Taylor. 2014. "CPT-based liquefaction assessments in Christchurch, New Zealand. In *Proc.*, CPT'14: 3rd Int. Symp. on Cone Penetration Testing, 13–14. Las Vegas: Organizing Committee of International Symposium on Cone Penetration Testing.
- Cao, Z., T. Youd, and X. Yuan. 2013. "Chinese dynamic penetration test for liquefaction evaluation in gravelly soils." J. Geotech. Geoenviron. Eng. 139 (8): 1320–1333. https://doi.org/10.1061/(ASCE)GT.1943-5606 .0000857.
- Cao, Z., T. L. Youd, and X. Yuan. 2011. "Gravelly soils that liquefied during 2008 Wenchuan, China earthquake, $M_s=8.0$." Soil Dyn. Earthquake Eng. 31 (8): 1132–1143. https://doi.org/10.1016/j.soildyn.2011.04.001.
- Chowdhury, K., E. Dawson, P. E. Camilo Alvarez, and R. B. Seed. 2021. "An end bearing method for evaluating instrumented Becker penetration test data for site characterization." In *Proc., USSD Annual Conf.* Aurora, CO: United States Society on Dams.
- Cubrinovski, M., J. D. Bray, C. de la Torre, M. Olsen, B. Bradley, G. Chiaro, E. Stocks, L. Wotherspoon, and T. Krall. 2018. "Liquefaction-induced damage and CPT characterization of the reclamations at Centerport, Wellington liquefaction-induced damage and CPT characterization of the reclamations at Centerport, Wellington." *Bull. Seismol. Soc. Am.* 108 (3B): 1695–1708. https://doi.org/10.1785/0120170246.
- Cubrinovski, M., J. D. Bray, C. De La Torre, M. J. Olsen, B. A. Bradley, G. Chiaro, E. Stocks, and L. Wotherspoon. 2017. "Liquefaction effects and associated damages observed at the Wellington Centerport from the 2016 Kaikōura earthquake." *Bull. N.Z. Soc. Earthquake Eng.* 50 (2): 152–173. https://doi.org/10.5459/bnzsee.50.2.152-173.
- DeJong, J. T., M. Ghafghazi, A. P. Sturm, D. W. Wilson, J. den Dulk, R. J. Armstrong, A. Perez, and C. A. Davis. 2017. "Instrumented Becker penetration test. I: Equipment, operation, and performance." *J. Geotech. Geoenviron. Eng.* 143 (9): 04017062 https://doi.org/10.1061/(ASCE) GT.1943-5606.0001717.
- Dhakal, R., M. Cubrinovski, J. Bray, and C. de la Torre. 2020a. "Lique-faction assessment of reclaimed land at Centerport, Wellington." Bull. N.Z. Soc. Earthquake Eng. 53 (1): 1–12. https://doi.org/10.5459/bnzsee .53.1.1-12.
- Dhakal, R., M. Cubrinovski, and J. D. Bray. 2020b. "Geotechnical characterization and liquefaction evaluation of gravelly reclamations and hydraulic fills (Port of Wellington, New Zealand)." Soils Found. 60 (6): 1507–1531. https://doi.org/10.1016/j.sandf.2020.10.001.
- Green, R. A., M. Cubrinovski, B. Cox, C. Wood, L. Wotherspoon, B. Bradley, and B. Maurer. 2014. "Select liquefaction case histories from the 2010–2011 Canterbury earthquake sequence." *Earthquake Spectra* 30 (1): 131–153. https://doi.org/10.1193/030713EQS066M.

- Harder, L. F. 1997. "Application of the Becker penetration test for evaluating the liquefaction potential of gravelly soils." In *Proc.*, *NCEER Workshop on Evaluation of Liquefaction Resistance*. Buffalo, NY: National Center for Earthquake Engineering Research.
- Holden, C., A. Kaiser, R. Van Dissen, and R. Jury. 2013. "Sources, ground motion and structural response characteristics in Wellington of the 2013 Cook Strait earthquakes." *Bull. N.Z. Soc. Earthquake Eng.* 46 (4): 188–195. https://doi.org/10.5459/bnzsee.46.4.188-195.
- Iqbal, M. S., P. K. Robertson, and D. C. Sego. 2004. Discrete element modeling of cone penetration testing in coarse grain soils. Edmonton, AB, Canada: Univ. of Alberta.
- Japanese Geotechnical Society. 1996. "Geotechnical aspects of the January 17, 1995 Hyogoken-Nambu earthquake." In Soils and foundations, Special Issue No. 1. Tokyo: Japanese Geotechnical Society.
- Kokusho, T., and Y. Yoshida. 1997. "SPT N-value and S-wave velocity for gravelly soils with different grain size distribution." Soils Found. 37 (4): 105–113. https://doi.org/10.3208/sandf.37.4_105.
- Lopez, S., X. Vera-Grunauer, K. Rollins, and G. Salvatierra. 2018. "Gravelly soil liquefaction after the 2016 Ecuador Earthquake." In Proc., Conf. on Geotechnical Earthquake Engineering and Soil Dynamics V, 273–285. Reston, VA: ASCE.
- Morales, C., C. Ledezma, E. Sáez, S. Boldrini, and K. Rollins. 2020. "Seismic failure of an old pier during the 2014 M_w8.2, Pisagua, Chile earthquake." *Earthquake Spectra* 36 (2): 880–903. https://doi.org/10.1177/8755293019891726.
- Morris, G., B. Bradley, A. Walker, and T. Matushka. 2013. "Ground motion and damage observations in the Marlborough region from the 2013 Lake Grassmere earthquake." *Bull. N.Z. Soc. Earthquake Eng.* 46 (4): 169–187. https://doi.org/10.5459/bnzsee.46.4.169-187.
- Rhinehart, R., A. Brusak, and N. Potter. 2016. Liquefaction triggering assessment of gravelly soils: State-of-the-art review. Rep. ST-2016-0712-01. Washington, DC: US Bureau of Reclamation.
- Robertson, P. K., and C. E. Wride. 1998. "Evaluating cyclic liquefaction potential using the cone penetration test." *Can. Geotech. J.* 35 (3): 442–459. https://doi.org/10.1139/t98-017.
- Rollins, K. M., S. Amoroso, G. Milan, L. Minerelli, M. Vassallo, and G. Di Giulio. 2020. "Gravel liquefaction assessment using the dynamic cone penetration test based on field performance from the 1976 Friuli earthquake." J. Geotech. Geoenviro. Eng. 146 (6): 04020038. https:// doi.org/10.1061/(ASCE)GT.1943-5606.0002252.
- Rollins, K. M., J. Roy, A. Athanasopoulos-Zekkos, D. Zekkos, S. Amoroso, and Z. Cao. 2021. "New dynamic cone penetration test

- (DPT)-based procedure for liquefaction triggering assessment of gravelly soils." *J. Geotech. Geoenviron. Eng.* 147 (12): 04021141. https://doi.org/10.1061/(ASCE)GT.1943-5606.0002686.
- Roy, J., and K. M. Rollins. 2022. "Effect of hydraulic conductivity and impeded drainage on the liquefaction potential of gravelly soils." *Can. Geotech. J.* 59 (11): 1950–1968. https://doi.org/10.1139/cgj -2021-0579.
- Seed, H. B., and I. M. Idriss. 1971. "Simplified procedure for evaluating soil liquefaction potential." *J. Geotech. Eng. Div.* 97 (9): 1249–1273. https://doi.org/10.1061/JSFEAQ.0001662.
- Seed, H. B., P. P. Martin, and J. Lysmer. 1976. "The generation and dissipation of pore water pressure changes during soil liquefaction." J. Geotech. Eng. Div. 102 (4): 323–346. https://doi.org/10.1061/AJGEB6.0000258.
- Seed, H. B., K. Tokimatsu, L. F. Harder, and R. M. Chung. 1985. "Influence of SPT procedures in soil liquefaction resistance evaluations." J. Geotech. Eng. 111 (12): 1425–1445.https://doi.org/10.1061/(ASCE) 0733-9410(1985)111:12(1425).
- Semmens, S., G. D. Dellow, and N. D. Perrin. 2010. It's our fault– Geological and geotechnical characterization of the Wellington Central Business District, GNS Science Consultancy Rep. 2010/176. Lower Hutt, New Zealand: Institute of Geological and Nuclear Sciences.
- Sy, A., and R. G. Campanella. 1994. "Becker and standard penetration tests (BPT–SPT) correlations with consideration of casing friction." *Can. Geotech. J.* 31 (3): 343–356. https://doi.org/10.1139/t94-042.
- Tokimatsu, K. 1988. "Penetration tests for dynamic problems." In *Proc.*, Int. Symp. on Penetration Testing; ISOPT-1, 117–136. Rotterdam, Netherlands: A. A. Balkema.
- Tonkin & Taylor. 2006. Harbor Quays development factual geotechnical report. Ref. No. 83725.004. Auckland, New Zealand: Tonkin & Taylor.
- Tonkin & Taylor. 2012. Thorndon container wharf seismic assessment geotechnical factual report. Ref. No. 85369.001. Auckland, New Zealand: Tonkin & Taylor.
- Tonkin & Taylor. 2014. Thorndon container wharf seismic assessment geotechnical interpretive report. Ref. No. 85369.001. Auckland, New Zealand: Tonkin & Taylor.
- Van Dissen, R., et al. 2013. "Landslides and liquefaction generated by the Cook Strait and Lake Grassmere earthquakes: A reconnaissance report." *Bull. N.Z. Soc. Earthquake Eng.* 46 (4): 196–200. https://doi.org/10.5459/bnzsee.46.4.196-200.